Initial Modeling of the August 2000 Houston-Galveston Ozone Episode

John W. Nielsen-Gammon
Department of Atmospheric Sciences
Texas A&M University

a report to the Technical Analysis Division,
Texas Natural Resource Conservation Commission
December 19, 2001

Contact Information:
John W. Nielsen-Gammon
Department of Atmospheric Sciences
3150 TAMU
College Station, TX 77843-3150
Phone: 979-862-2248 Fax: 979-862-4466
Email: n-g@tamu.edu

Summary

This report describes MM5 modeling work to date at Texas A&M University, sponsored by the Texas Natural Resource Conservation Commission, with the goal of an accurate, fully validated meteorological simulation delivered by February 28, 2002. Specifically, this report describes the meteorological conditions during the August 25-September 1, 2000, Houston-Galveston ozone episode, describes the modeling philosophy being followed to develop high-quality meteorological fields, describes the MM5 modeling system itself, and describes the results of various experiments conducted over the past few months.

Results so far indicate that, with suitable modification to land surface and/or radiative forcing, the MM5 is fully capable of simulating the temperatures and vertical extent of the daytime boundary layer. Low-level nighttime temperatures are too warm, which may lead to overly robust turbulent mixing at night. The present nesting scheme produces very good quality large-scale winds and realistic sea breeze evolution.

Future work will focus on determining the accuracy of the model-simulated nighttime wind cycle, and, if necessary, investigating ways of improving the nighttime winds. Differences in behavior of various PBL schemes will be further investigated and evaluated. Wind profiler and Doppler lidar data will be assimilated on a coarse scale, and statistical measures of model accuracy will be used to provide objective measures of model performance.

Of all model runs that have been conducted so far, the best performance has been exhibited by the dec6grid4 run, with the MRF planetary boundary layer scheme and an extra sigma layer near the ground.

Table of Contents

List of Figures

FIGURE 13: Ten-meter winds (scaled to represent one-hour transport) and short wave radiation reaching the surface (W/m**2, low values imply clouds), 18 UTC August 25, 2000, from the sept24grid4redux simulation.

FIGURE 14: Winds and shortwave radiation, 18 UTC August 25, 2000, as in Fig. 13, except from the aug31 simulation.

FIGURE 15: Temperatures (F; 2 m above ground) and surface winds (10 m above ground), 21 UTC August 31, 2000, from the sept24grid4redux simulation. Wind plotting convention as in Figs. 1-8.

FIGURE 16: Temperatures and winds, 21 UTC August 31, 2000, as in Fig. 15, but from the aug31 simulation.

FIGURE 17: Incoming shortwave radiation and winds, 18 UTC August 25, 2000, as in Figs. 13 and 14 except from the oct25grid4 simulation.

FIGURE 18: Surface temperatures and winds, 21 UTC August 31, 2000, as in Figs. 15-16 but from the oct25grid4 simulation.

FIGURE 19: Locations of National Weather Service regular observing stations in Houston and surrounding areas. Green stations are treated collectively as Houston area stations (not pictured: 11R, located west of DWH and south of CLL); blue stations are coastal plain stations, and brown stations are inland stations.

FIGURE 20: Comparison of hourly maximum and minimum temperatures averaged from eight station locations in the Houston area with two model forecasts. Successive groupings of data, from left to right, are maximum temperatures, August 23, 2000, minimum temperatures, August 24, maximum temperatures, August 24, etc.

FIGURE 21: Stuve diagram, 23 UTC August 30, 2000, Wharton Power Plant rawinsonde launch site. Green: rawinsonde observations of dewpoint and temperature (Celsius). Light blue: dec14grid4 simulation (default soil moisture). Brown: dec7grid4 simulation (basic soil moisture). Yellow: dec16grid4 simulation (dry soil moisture). Red: oct25grid4 simulation (basic soil moisture, MRF PBL). Background lines are, clockwise from horizontal, pressure (mb, black), potential temperature (red), equivalent potential temperature (green), saturation mixing ratio (blue), and temperature (C, black).

List of Tables

1. Introduction

Texas A&M University, through the Texas Engineering Experiment Station, has been tasked with developing meteorological model fields that can be used to drive photochemical model simulations of ozone development in the Houston-Galveston area. The period of simulation includes August 25, 2000 through September 1, 2000, which includes a portion of the Texas 2000 Air Quality Study (TexAQS 2000) field program. Specifically, for the purposes of this report, Texas A&M will:

(a) Format and quality assure surface meteorological data and TexAQS 2000 profiler, GPS sonde, and Airsonde data for MM5 modeling, in coordination with other TexAQS researchers;

(b) Incorporate new features to improve MM5 modeling, including alteration of land surface characteristics;

(c) Develop three-dimensional analysis fields with TexAQS 2000 data, including assimilation of appropriate special observations with the MM5 forecasted wind fields;

(d) Perform performance evaluation of the MM5 model runs.

Task (a) in the above list is complete. Tasks (b) and (c) are iterative in nature, with repeated tests and fine-tuning as the work proceeds. Task (d) is continuous and ongoing. Also, additional meteorological analysis has been performed with the aim of understanding the nature of model errors and and the processes responsible for them, so that to the greatest extent possible the MM5 can be modified to cure the source of the errors rather than merely mask them.

The final delivery date for the modeling runs and documentation is Feb. 28, 2002. This report documents the progress up to this date, describes the experiments that have been performed, and documents the settings and characteristics of the model runs.

The organization of this report is as follows. Section 2 describes the meteorological characteristics of the ozone episode, using regular and special observations collected during TexAQS-2000. Section 3 describes the modeling protocol that is being followed, including model analysis and validation techniques. Section 4 describes the basic model setup for the experimental runs. Section 5 describes the results of numerical simulations that have been performed to date. The conclusions are listed in Section 6, along with a description of future work.

2. Meteorological Conditions During the August 2000 Ozone Episode

2a: Overview of Houston/Galveston summertime meteorology

Houston is located close to the Gulf of Mexico, just south of 30 N. To the west and southwest, the Mexican High Plain produces a barrier to low-level flow, causing winds to be predominantly from the south or north rather than the east or west. Weather is characteristic of midlatitudes during the cold season and of the tropics during the warm season. The climatological conditions support a variety of ecosystems in the Houston area, including coastal marshes, prairie, oak savannah, and pine forests.

Weather conditions in southeast Texas during summertime are typically hot and muggy, with occasional thundershowers. The predominant wind direction is from the southeast, associated with the western edge of the Bermuda High. This anticyclone typically weakens during the latter part of the summer, leading to lighter and more variable winds. High temperatures are typically 30-36 C during the second half of August and the first half of September; low temperatures range from 20-25 C.

Precipitation is variable, and can be associated with afternoon thunderstorms along the sea breeze front or more widespread thunderstorm activity associated with tropical disturbances or tropical cyclones. Average monthly precipitation during August and September is 75 mm to 150 mm.

2b: Meteorological conditions during the 2000 warm season

The summer of 2000 was exceptional for southeast Texas. In early September of 2000, many locations set records for the highest temperature ever recorded. These events were brought on by widespread drought during the preceding few months.

Table 1 shows the monthly weather records during the period May 2000 through September 2000. Following a wet spring, drought conditions set in by June. All stations received well below normal precipitation during June, July, and August. Significant precipitation in September was not received until Sept. 13.

The dry conditions are consistent with the increased spread between the maximum and minimum temperatures. This effect can be caused by both a decrease in cloud cover and a decrease in absolute humidity, both of which were observed during the period. Although minimum temperatures were near or slightly below normal, maximum temperatures were well above normal. The warmer daytime temperatures in turn caused increased potential evaporation from the ground and from vegetation, further contributing to dry soil conditions across southeast Texas.

2c. Meteorological conditions during the August 2000 ozone episode

This subsection summarizes the weather conditions and their apparent impact on ozone formation during August 23, 2000 (8/23) through September 1, 2000 (9/1). Throughout the remainder of the paper, dates will be abbreviated as above. The discussion begins on 8/23 because, as discussed in Section 3, the model simulations of the ozone episode begin on that date.

TABLE 1: Departures from normal (degrees Celsius) and percentage of normal precipitation, May-September 2000 (source: National Weather Service)

		May	June	July	Aug	Sept
Houston Intercontinental						
	MAX	1.3	0.2	2.8	2.7	2.1
	MIN	2.7	0.9	0.2	0.1	-0.7
	PRECIP	236	66	18	60	89
Galveston						
	MAX	2.1	1.6	1.8	2.1	1.8
	MIN	1.4	0.8	-0.2	0.1	-0.8
	PRECIP	128	25	24	28	106
Beaumont/Port Arthur						
	MAX	0.5	0.2	1.4	2.0	1.9
	MIN	2.4	0.6	-0.3	-0.2	-0.4
	PRECIP	155	46	44	17	49
College Station						
	MAX	1.7	-0.1	3.3	3.6	3.8
	MIN	1.6	0.6	-0.8	-0.8	-1.2
	PRECIP	116	69	0	9	31

Table 2 shows the hourly average ozone characteristics from 8/23 through 9/1. The ozone on both 8/23 and 8/24 were limited by thunderstorms that developed during the late morning. On 8/23, the thunderstorms formed along the sea breeze and bay breeze front. On 8/24, a broad area of thunderstorms developed east of Houston and moved westward across the metropolitan area.

TABLE 2: Ozone exceedances during August 2000 episode (source: Texas Natural Resource Conservation Commission)

	Highest hourly average ozone (PPBV)	Number of stations exceeding 124 PPBV
8/23	101	0
8/24	111	0
8/25	194	12
8/26	140	1
8/27	87	0
8/28	122	0
8/29	146	3
8/30	199	7
8/31	168	10
9/1	163	2

The high ozone episode began on 8/25 with stagnant conditions during the late morning which apparently allowed an area of high ozone to develop in the Ship Channel area and move westward during the day. Figure 1 shows the surface winds, temperatures, dewpoints, and ozone levels at 18 UTC (1 PM CDT, 12 Noon CST), at about the time

when the mass of air rich in ozone and its precursors had begun to move. Temperatures are generally in the upper 80s (Fahrenheit), and winds are generally from the east and rather light. The day was devoid of significant thunderstorm activity. More sites experienced exceedances on this day than on any other day during the episode.

The following day (8/26, Fig. 2), midday winds were light from the southeast rather than the east. The highest ozone on the map is northeast of the Ship Channel, and stations west of the Ship Channel are nearly 100 PPB lower than on the previous day. Aircraft observations indicate that moderately high ozone was reached northeast of Houston on this day but was largely unobserved by fixed surface sensors. No precipitation was observed in southeastern Texas.

On 8/27 (Fig. 3) and 8/28 (Fig. 4), noontime winds were well organized and from the southeast on both days. During the preceding mornings, winds had become light but not calm, and ozone values remained below legal limits. The highest ozone values were generally observed late in the day at Conroe, well north of Houston. There was no precipitation in eastern Texas on either day.

A stealth ozone day occurred on 8/29 (Fig. 5), in the sense that aircraft observations of a high ozone event over the northern part of Galveston Bay were matched by surface observations of a mere moderate ozone event. At 18 UTC, winds were generally light and disorganized throughout the area. By 21 UTC (not shown), they would be systematically from the southeast, much like on the previous few days. Again, the day was free of precipitation. Temperatures by 18 UTC on 8/29 were in the low to mid 90s everywhere except along the immediate coastline, following a slight warming trend over the previous few days.

Conditions on 8/30 and the following two days are shown at 21 UTC, or midafternoon, because winds tended to be lightest during the afternoon on those days and the highest ozone was typically observed during late afternoon. On 8/30 (Fig. 6), winds are light and disorganized over land, while coastal stations report the onshore flow of a bay breeze or gulf breeze. Very high ozone is found at LaPorte and Texas City, with the highest totals found behind the sea breeze front. Winds during the previous hours were from the west and northwest, presumably advection Houston emissions over Galveston Bay to be carried back over land during the afternoon bay breeze. This view of the day is consistent with airborne ozone lidar measurements by the Environmental Technology Laboratory of the National Oceanographic and Atmospheric Administration (NOAA/ETL). The day was again free of precipitation. The highest hourly average ozone of the episode occurred on this day.

The following day, 8/31 (Fig. 7), also had relatively calm winds during the afternoon. On this day, the high ozone was not confined to the coast, but instead affected ten observing stations in central and eastern Houston. Temperatures had by this day climbed to unusually high levels, exceeding 100 Fahrenheit except along the immediate coast. During the late afternoon, thunderstorms developed over Louisiana and extreme eastern Texas. The thunderstorms dissipated after sundown, and a convective outflow boundary approached Houston from the northeast but did not reach the metropolitan area.

The final day of the ozone episode was 9/1. At 21 UTC (not shown), the winds were predominantly from the southwest everywhere and the highest ozone was downwind of the city. An organized area of thunderstorms had developed north and east of Houston and was moving southwestward rapidly. By 23 UTC (Fig. 8), the outflow

from the thunderstorms had reached the center of Houston, dropping temperatures to the 80s and 90s and bringing strong winds from the north and northeast. Ahead of the cold thunderstorm air, temperatures remained in the 100s.

On days following the episode, winds remained largely from the west; the lack of an interval of calm winds apparently contributed to the lack of extremely high ozone. However, ozone exceedances were observed on all days through 9/6.

2d: Meteorological regimes during the August 2000 ozone episode

2d.1) Overview

We have performed preliminary analyses of much of the profiler, surface, and buoy data from TexAQS 2000. Initial results, reported at the August 2001 TexAQS workshop in Austin, TX, showed that on days without widespread convective activity the winds followed a regular diurnal (one-day) cycle. This cycle was observed far offshore and aloft as well as along the coast, and featured the strongest onshore (toward land) winds during the evening and the strongest offshore (toward water) winds during the morning. Theoretical studies, by Richard Rotunno and others, attribute this behavior to the interaction with the sea breeze and the Earth's rotation at a latitude where the so-called inertial period is slightly greater than one day. The development of a local bay/gulf breeze along the coast can be viewed as a nonlinear modification to the much broader-scale diurnal wind cycle.

Subsequent analysis by us during October and November 2001 indicates that the behavior of the wind during these undisturbed days is extremely sensitive to whether the large-scale wind is onshore or offshore. The August 2000 ozone episode included both types of days: large-scale onshore flow was present Aug. 25-29, while winds parallel to the coast or offshore were present Aug. 30-Sept. 1. Composites of winds on these days were similar to composites drawn from the entire TexAQS 2000 period, so the nature of these regimes will be discussed by reference to composites from the ozone episode.

2d.2) Regime I

Fig. 9 is a composite of winds at Houston Southwest Airport wind profiler site for Aug. 25-29. We shall call this period Regime I. This and the composite in Fig. 10 were constructed from data which had not been filtered for bird contamination; such filtering indicates that winds below 800 m are uncontaminated. The contamination is limited to nighttime hours. The composites shown are similar to composites of data from other profiler sites.

The composite shows that the time hodograph traces out a nearly perfect circle at most levels. There is a slight time lag of 1-2 hours from the ground to 1000 m, but the amplitude of the wind variation is nearly constant with height. As a result, the composite shows very little vertical wind shear.

A comparison with linear theory suggests aspects of this wind pattern that may be sensitive to certain aspects of a meteorological model. The amplitude, or size, of the circle is determined by the amount of daytime heating and nighttime cooling, so proper simulation of the diurnal temperature cycle over land will be an important aspect of the

simulation. The location of the circle on the hodograph depends on the strength and direction of the large-scale winds. The slight time lag with height in the observations is inconsistent with theory, which predicts that the latest phase in the cycle should happen at the ground. We hypothesize that this discrepancy is due to the difference in the timing of heating as a function of altitude: in linear theory the heating occurs simultaneously throughout the planetary boundary layer (PBL), while in the real atmosphere the heating occurs later and later with height as the PBL deepens during the day. Correct modeling of the growth of the PBL will be important to simulating the vertical structure of the diurnal wind cycle.

2d.3) Regime II

In contrast, Fig. 10 shows the composite winds at the Houston Southwest Airport profiler site for Aug. 30-Sept. 1. We call this period Regime II. Instead of a regular circle, the hodograph trace is an elongated ellipse; instead of similar wind variations with height, the diurnal cycle decays to near zero by a height of 1 km; and instead of a wind variation of a few m/s, the wind changes by more than 10 m/s on average between sunset and sunrise. A fourth difference, that most of the winds are westerly rather than southerly, is attributable to the large-scale wind being from the west rather than the south.

We hypothesize that the other differences between Regime I and Regime II are a consequence of the different large-scale wind direction (or, more precisely, the geostrophic wind direction). In particular, the coast-parallel winds allowed temperature to reach very high values during Regime II. The resulting land-sea temperature gradient caused a drop in pressure at low levels over land and a situation known as adverse shear, in which the balanced wind is strongest at low levels and decreases or reverses direction aloft. Such an adverse shear is seen by comparing low-level and 1-km winds in Fig. 10: the average wind at low levels is from the WSW at about 6 m/s, while the average wind at 1 km is nearly zero.

Adverse shear is a classic indicator of nocturnal low-level jets, for the following reason: during daytime, the well-mixed PBL causes winds to be homogenized throughout the lowest 2 km or so of the atmosphere. Since the large-scale wind speed decreases with height, the average wind in the lowest 2 km is much weaker than what the surface wind would otherwise be. Thus, during the day, friction acts to slow the wind even more than it would in the absence of wind shear. At night, when a surface temperature inversion develops in response to radiational cooling, the winds aloft decouple from the surface. No longer feeling the retarding effect of friction, they accelerate, and in fact overshoot much like a pendulum bob released from one side swings across to the other side. The acceleration is strongest near the ground because the effect of friction was strongest there and the pressure gradient is strongest there as well.

At the surface, while this acceleration is going on aloft, the air is trapped by the inversion to remain near the ground, and winds remain very light. During the morning, as the PBL deepens, the strong winds of the low-level jet mix down to the surface, and surface winds increase for a few hours until the PBL gets deep enough to include the lighter winds aloft. As the mixing takes place, the low-level jet weakens rapidly. This mechanism is dynamically similar to the mechanism which drives the Great Plains summertime low-level jet.

We further hypothesize that the magnitude of the low-level jet is locally enhanced by the additional effect of the diurnal heating cycle. Essentially, the frictionally induced wind cycle is almost exactly in phase with the sea breeze wind cycle, so that the two effects amplify each other.

2d.4) Significance of the diurnal wind cycle

The diurnal wind cycle is crucial for understanding the evolution of the surface winds during a high ozone day. For days in Regime I, a large-scale wind of close to 3 m/s, such as is found in the composite, would lead to a few hours in which the wind becomes calm and gradually reverses direction. Such an event took place on 8/25. Other days, when the large-scale wind is slightly stronger, should see no stagnation events and as a result less ozone. When the large-scale wind is from the south, the stagnation should take place between 9 AM and noon LST. Very light large-scale winds might cause one day's emissions to execute a complete loop and return to the city on the following day.

In contrast, Regime II days, with appropriate large-scale winds, reach stagnation during the afternoon. At night, the large vertical shears would redistribute ozone horizontally, with air at different levels moving to different places. At an altitude where the winds are light, the ozone might stay in place to help elevate ozone levels the following day, but the impact should not be as great as if an entire column of air from the previous day was present at one location.

3. Procedure for Developing the MM5 Simulations

3a: The MM5 Model

In this document, MM5 refers to the NCAR/Penn State (National Center for Atmospheric Research/The Pennsylvania State University) Mesoscale Model, Version 5, Release 3.4. The MM5 is a state-of-the-art mesoscale model designed for phenomena originally designed for model simulations of one or two days with grid spacings of 30 to 80 km. The model has evolved to include a sophisticated set of parameterizations which allow the model to be run realistically on scales larger than boundary layer turbulence (a few km) all the way to global climate simulations. Documentation for the model exists in technical memoranda and articles, but the most current documentation is available online at http://www.mmm.ucar.edu/mm5/mm5-home.html in the form of tutorial notes, descriptions of model updates, and other documents.

The MM5 is one of several models presently being used for high-resolution (<10 km grid spacing) mesoscale simulations, and along with the CSU-RAMS model, is one of the most widely used mesoscale models in the world. The model is appropriate for simulating winds and temperatures across a metropolitan area over a several-day period, as it is being used here. The MM5 is accepted for use for regulatory purposes by the Environmental Protection Agency, and, perhaps not insignificantly, it is the only numerical model with which the author of this report has extensive firsthand experience. The MM5 has been used at Texas A&M University to study phenomena such as urban heat islands, slantwise convection, extreme rainfall events, and drylines. During the TexAQS 2000 field program, Texas A&M operated the MM5 in forecasting mode, producing predictions for southeast Texas at 4 km grid spacing up to 36 hours in advance.

The MM5, as presently configured, is a non-hydrostatic, sigma coordinate (terrain-following) atmospheric model with optional land surface model interfaces. The MM5 modeling system includes the MM5 model itself as well as various ancillary programs for, among other tasks, establishing the model grid configuration, initial and boundary conditions, and land surface characteristics. All such programs used in the project are the most recent available as of the summer of 2001.

The MM5 is modified slightly from its release version to fix a bug in the output software (see Section 5a). This bug, according to NCAR, did not affect the model integration itself, only the timing of output.

For the purposes of model validation and graphical inspection of model output, additional postprocessing programs were developed by Texas A&M University for converting MM5 output into Gempak format. Gempak is a freely-available meteorological display software package developed by the National Aeronautical and Space Administration and the National Weather Service.

3b: The Modeling Environment and Output Locations

All model runs are conducted on typhoon, a sixteen-processor SGI Origin operated by TNRCC. Postprocessing is performed on typhoon and locally at Texas A&M University. All work is performed on `/met/ngammon`, with subdirectories organized as follows:

`data`: Observations from the TexAQS-2000 field program.
`analyses`
- `ncar`: Eta Data Assimilation System gridded analyses
- `terrain`: Output and control files from the TERRAIN MM5 preprocessor
- `pregrid`: Output and control files from the PREGRID MM5 preprocessor
- `regridder`: Output and control files from the REGRIDDER MM5 preprocessor
- `interpf`: Output and control files from the INTERPF MM5 preprocessor

`mm53.4`: The MM5 and preprocessor programs and runtime directories
`output`: Output files from the MM5 program, software to manipulate and convert them, and converted files. Within output, model runs are in subdirectories which are named according to date of completion and grid number.
`gempak`: Gempak software and executables
`verif`: Verification software and verification output files

In this document, model runs will be referred to by their subdirectory name within /met/ngammon/output.

A complete model run begins with specification of the grid dimensions in the TERRAIN program. Following this step, gridded analyses are converted (PREGRID) and horizontally and vertically interpolated (REGRIDDER) to the model grid in pressure coordinates. Then, an optional objective analysis may be performed using the REGRIDDER output as a first guess (RAWINS or little_r). Next, the analyses and TERRAIN output are converted to initial conditions, boundary conditions, and optional nudging grids (in sigma coordinates).

The programs RAWINS and little_r are not being used for the ozone episode modeling. The original purpose of these programs was to allow the initially coarse analysis fields to be enhanced by a univariate analysis with available data. Instead, we are using analysis fields which are already high-resolution. Model runs are commencing two days before the onset of the episode, so any small-scale features in the initial conditions will have vanished by 8/25. Special TexAQS data to be incorporated directly into the model simulation will be assimilated through nudging. In summary, a separate objective analysis step is at best superfluous and is likely to be detrimental, since the analysis procedures in the MM5 preprocessors are much less sophisticated than the analysis schemes used to derive the initial analyses.

3c: Procedure for Developing Model Improvements

3c.1) Basic philosophy

During TexAQS-2000, a wide range of regular and special meteorological observations were taken. This data set will make it possible to obtain more accurate simulations of the wind and temperature fields in the Houston area than ever before.

Meteorological observations can be used in two ways. First, observations may be used to validate the model and determine the accuracy of the modeled fields. This process may be iterative, in the sense that the model characteristics may be altered so as to improve the agreement between the observations and the modeled fields. Second, observations may be assimilated into the model to directly improve the accuracy of the modeled fields.

There are multiple ways of attempting to obtain modeled wind and temperature fields that match the observations as closely as possible. Three such techniques are described now. In comparison to observations, the resulting fields, obtained by different methods, may be indistinguishably accurate, but the modeled fields are likely to be considerably different where observations do not exist.

The preferred technique is to refine the model so that it accurately simulates all the important processes occurring in nature. These processes may be simulated directly or through parameterizations. In general, there are many paramerizations available, and each parameterization has a variety of settings which can be adjusted to better allow the parameterization to mimic the particular physical environment of the simulation. If observations provide direct evidence that a particular parameterization is deficient in one or more aspects, an adjustment of the parameterization to fix the deficiency will also fix all model errors that are caused by that deficiency. This technique, while preferred, is difficult and generally requires extensive specialized observations.

The second best technique is to refine the model so that it accurately reproduces the results of important processes occurring in nature. This process is distinct from the preferred technique because the appropriate aspects of the model may not necessarily be adjusted. Instead, an inaccuracy may be introduced which compensates for another inaccuracy inherent in the model. If such compensating errors are introduced, it is desirable to introduce them as early in the cause-and-effect chain of events as possible, so that meteorological fields of particular interest do not contain these errors.

The third, and least preferred, technique is to assimilate data into the model simulation, through techniques such as data nudging. In principle, there is nothing inherently wrong with this procedure, but for it to work properly with the current version of MM5 the observations must be sufficiently well distributed so as to fully represent the phenomena of interest. In most realistic circumstances, the data are far from being well distributed, and data assimilation may instead cause little improvement, no improvement, or even degrade the model simulation away from the observations.

To take one relevant example, consider a model forecast of a sea breeze front in which the simulated front moves inland too slowly. In the MM5 model, this failure can have many causes, one of which would be too strong an opposing wind over land. The preferred technique for fixing this problem would be to identify the cause of the opposing wind error (for example, an incorrect analysis being assimilated on the large-scale grid) and correct it. A less optimal technique would be to decrease the surface heating over land so that the modeled sea breeze advances more slowly. This technique would get the right answer for the wrong reasons, and would still retain the inaccuracies of the wind field ahead of and above the sea breeze. The least optimal technique would be to

assimilate surface temperature observations that include the passage of the sea breeze front. In the MM5 assimilation scheme, such a procedure would likely lead to discontinous propagation of the sea breeze front or destruction of the front entirely, because the observations are being assimilated on a scale much larger than that of the sea breeze front. Under that circumstance, while the model will agree more closely with the surface temperatures, it will suffer in its ability to accurately represent the remainder of the three-dimensional atmosphere within its domain.

3c.2) Simulation of the diurnal cycles

A consistent theme in the above discussion is that proper refinement of the model requires knowledge of the processes that lead to model error. According to the meteorological analysis in Section 2, the most important model processes for simulating winds on high ozone days in Houston are those processes which drive the diurnal cycles of wind, temperature, and moisture. Rather than assimilate observations directly into the MM5 simulation, a model configuration and lower boundary conditions will be identified that allow the model to accurately simulate the diurnal cycles.

The sea breeze in the Houston-Galveston area includes two basic phenomena. The first is the sea breeze front, which develops near the coastline during light or onshore wind conditions and propagates inland as a density current, with onshore flow in the lowest km or so of the atmosphere and return flow aloft. The second is the large-scale diurnal wind oscillation, which takes the form of a nearly simultaneous clockwise rotation of the wind vector on a hodograph over broad areas of southeast Texas and the adjacent Gulf of Mexico. This latter phenomenon has a rich vertical structure and is a consequence of the near-resonance between the diurnal sea breeze forcing and the local inertial period. Both phenomena are controlled by the land-sea temperature difference and the larger-scale wind, and interact with convection, the urban heat island, and other local phenomena.

If the model simulation of the sea breeze is poor, conventional data nudging will do little to help it. Observation error will be greatest where the model has an erroneous sea breeze front location. However, wind nudging will not correct the sea breeze front location; instead, it will artificially displace the sea breeze into or out of a circular region around the observation while substantially weakening the sea breeze front itself. Furthermore, except for two or three locations near the coast with wind observations distributed vertically, the vertical structure of the nudged sea breeze will depend strongly on the vertical structure of the nudging coefficient rather than the sea breeze dynamics itself. Similarly, temperature nudging will artificially alter the temperature field near the sea breeze front, producing artificial, discontinuous sea breeze motion and permanently distorting the sea breeze structure.

The model simulation of the sea breeze will be improved by altering the forcing of the physical processes that produce the sea breeze. Existing land surface categories may be altered by adjusting the moisture availability, the albedo, and other characteristics. Additional land surface categories may be created to represent transitional land use types between the urban and agricultural categories that dominate in the Houston area. Characteristics can even be altered on a grid point basis based on remotely-sensed satellite data or airborne thermal imagery.

Unlike observational nudging, which alters directly observed fields in the model, representative land surface characteristics in the Houston area are essentially unobserved. However, there are ample observations of the effect of the land surface characteristics and their variations. These observations are of the diurnal surface temperature cycle, of the vertical structure of the boundary layer (determined by soundings and aircraft ascents/descents), and of the sea breeze strength, structure, and evolution. Assuming that the MM5 is dynamically able to simulate the sea breeze if given the proper forcing, the observations of the land surface effects will be used to tune the land surface characteristics so as to allow the model to reproduce both the diurnal temperature cycle and the sea breeze cycle in a dynamically consistent, realistic way. Depending on the outcome of this work, it may also prove useful to nudge surface temperatures toward the observational network, to the extent that the intra-network temperature variations are judged to be realistic.

The meteorological analysis in Section 2 also noted that the second portion of the August ozone episode, Regime II, involved winds that were likely to be sensitive to low-level grid structure and the planetary boundary layer parameterization. If the vertical mixing of momentum is not properly handled in the model, the resulting diurnal wind cycle will be incorrect even if the surface temperature cycle is correct in the MM5. If a deficiency is found in the momentum mixing, the PBL parameterization may be specifically altered to reduce the mixing to a level commensurate with observations, given the observed response of the low-level winds in the profiler and Doppler lidar data.

3c.3) Large-scale nudging of mesoscale observations

In addition to the local forcing, the diurnal sea breeze cycle is also sensitive to the large-scale ambient winds. The large-scale flow strongly affects the position and timing of the sea breeze and moderately affects the strength of the sea breeze front itself. Of course, the large-scale winds also directly impact transport of ozone and its precursors. The large-scale wind field will be constrained fairly tightly by the analysis nudging being performed on the coarser grids, which directly affects the boundary conditions of the finer meshes. However, within the finest mesh, simple nudging of the wind field, from profiler and other data, will detrimentally affect the sea breeze structure itself, for reasons discussed above. Thus, it is important that the land surface characteristics be optimized before wind data nudging is attempted.

The wind data takes two forms. Some data has very high vertical resolution but is only available at a handful of locations. Other data is widely available but consists only of surface data. This first class of data, consisting mostly of profiler observations (including Doppler lidar wind profiles), is well suited for determining the large-scale three-dimensional wind structure. The second class of data, consisting mostly of anemometers a few meters above the ground, is not suited for measuring large-scale wind speed and direction (because the measurements are strongly sensitive to the land surface characteristics in the immediate vicinity) but with appropriate caution can provide useful information on smaller-scale horizontal wind field variations. (A third type of data is aircraft flight-level winds; nudging to flight-level winds is problematic and to our knowledge has never been attempted within a high-resolution mesoscale model.)

The profiler wind observations will be utilized in a nudging framework that allows the profiler data to affect only the large-scale winds in the model while leaving the smaller-scale winds intact. Possible procedures for doing so include using nudging weighting functions which decay very slowly away from the observations and performing temporal averaging of the profiler observations, the model simulations, or both, before computing observation increments. As a separate, final step, additional small-scale nudging of the boundary-layer winds, based on surface observations, may be employed in the (hopefully) unlikely event that significant model discrepancies remain.

3c.4) Fine tuning

Once the diurnal cycle and large-scale winds are simulated correctly, other model adjustments will be made to fine-tune the simulation. It is difficult to go into much detail at this point, since it is not known ahead of time what will cause the remaining errors.

One possible source of error is convection. In simulations of this and previous ozone events, the MM5 has been shown to be susceptible to apparently unrealistic large-scale convective cells, which produce broad downdrafts within the boundary layer. Since we will not be coupling the MM5 to a true land surface model, the clouds and precipitation will not alter the soil moisture, and therefore will not have a significant permanent effect on the simulation. However, to the extent that the convective cells are forecast to occur in locations where observations indicate both no convection and high ozone (or its precursors), this problem may require attention. It is not known ahead of time whether the problem will still exist after appropriate land surface characteristics are determined. If it does, it may be necessary to modify the model in other ways, for example by selectively or globally eliminating or reducing parameterized evaporative cooling.

3c.5) Model validation

The model development and improvement activities described above involve independent treatment of the diurnal sea breeze cycle, the large-scale winds, and the smaller-scale winds. Consequently, a model validation procedure must be established that makes it possible to distinguish among these different types of error. Essentially, this amounts to a combination of statistical and phenomenological validation.

Initial model validation will focus on the diurnal cycles. Important aspects of the simulation will be accurate representation of the diurnal heating cycle over land, including fluxes of heat, moisture and radiation, as determined by changes in the temperature and moisture of the boundary layer. Important elements of the wind field include proper simulation of the diurnal wind cycle as a function of location and height. The wind field validation, in particular, will be qualitative in nature, because many processes besides errors in the diurnal cycle can lead to wind errors.

When nudging to profiler winds begins, it will be difficult to measure the improvement in the three-dimensional wind field. Data will be withheld in order to measure the improvement (if any) in the simulations at locations where observations were not assimilated. Also, one important indicator of the accuracy of the assimilation is the motion of the sea breeze front. The progression of the front is sensitive to the large-scale

winds and will not be resolved by the filtered profiler observations, so an improvement in the frontal motion is independent evidence of improvement in the large-scale winds.

During the final stage of validation, statistical validation measures will be used extensively. We plan to use the MAPS software package, provided to Texas A&M and TNRCC by Dennis McNally and Tom Tesche of Alpine Geophysics. In addition to recommended statistical measures of model performance, we will estimate errors in "wind run", the lateral displacement of air as measured by its motion past a station. This measure is an excellent way of estimating likely errors in air parcel trajectories from point observations alone. Such errors in the meteorological fields are likely to cause errors in the placement and magnitude of ozone concentrations, so it is important to document and understand the uncertainty in the model trajectories.

Finally, as an aid to model assessment, we will use trajectories of parcels emitted from known pollution sources to infer the likely location of high ozone air according to the MM5 model simulations. The primary purpose of this procedure will be to understand the likely sensitivity of air parcel trajectories to various changes in the configuration of the MM5 model. A secondary benefit of this procedure will be to provide information on alternate model run output should initial photochemical model experiments produce significant placement errors.

3c.6) Use of conventional and special data

The modeling philosophy outlined above makes heavy use of the data collected during the TexAQS 2000 field program. Indeed, this approach would not be possible without the field program data. Only because of the special observations do we know the vertical structure of the sea breeze cycle, the enhanced low-level jet during alongshore wind conditions, the horizontal structure of these phenomena, and the relationship between the low-level wind maxima and nocturnal temperature inversions. Because these critical phenomena are well observed, it will be possible to analyze deficiencies in the MM5 configuration and (hopefully) correct them so that the model is able to reproduce the basic structure, timing, and amplitude of the daily wind cycle. Ideally, the MM5 will be made to perform so well that data assimilation would be unnecessary. In practice, we will work to make the MM5 simulation as realistic as possible and use data assimilation selectively to compensate for any remaining unrealistic features.

4. Basic Model Setup

4a: Introduction

This section describes the configuration of the MM5 model and its preprocessors for the basic MM5 model simulation of the August 2000 ozone episode. The basic model run serves as a useful point of departure for discussion of other model experiments. Of the various model runs that have been conducted to date, the basic model run is so identified because it is most similar to the other model runs in its configuration; most other model runs differ in only one or two aspects from the basic model run.

4b: TERRAIN Configuration Parameters

All MM5 simulations use a grid configuration for 108 km, 36 km, 12 km, and 4 km grids originally proposed by TNRCC and adopted by Texas A&M University as reasonable and scientifically justifiable, except that the 4 km grid had to be altered slightly to conform to MM5 constraints. A fifth grid, with a 1 km grid spacing, is additionally specified in the event that such high resolution in the MM5 winds produces an improvement in the meteorological or photochemical simulations. The grids are defined with respect to a Lambert Conformal map projection centered at 40N, 100W. The configuration of the grids is shown in Fig. 11, and they are specified as follows:

```
MAXNES =    5,        ; NUMBER OF DOMAINS TO PROCESS
NESTIX =   43,   55,  100,  136,   133, 221,  ; GRID DIMENSIONS IN Y DIRECTION
NESTJX =   53,   55,  100,  151,   141, 221,  ; GRID DIMENSIONS IN X DIRECTION
DIS    =  108.,  36.,  12.,  4.0,  1.0, 1.0,  ; GRID DISTANCE
NUMNC  =    1,    1,    2,    3,    4,   5,  ; MOTHER DOMAIN ID
NESTI  =    1,    6,    6,   17,   43,  50,  ; LOWER LEFT I OF NEST IN MOTHER DOMAIN
NESTJ  =    1,   24,    8,   25,   49,  50,  ; LOWER LEFT J OF NEST IN MOTHER DOMAIN
NTYPE  =    1,    3,    4,    6,    6,   6,  ; INPUT DATA RESOLUTION
;
;      1:  1 deg (~111 km) global terrain and landuse
;      2: 30 min ( ~56 km) global terrain and landuse
;      3: 10 min ( ~19 km) global terrain and landuse
;      4;  5 min (  ~9 km) global terrain and landuse
;      5;  2 min (  ~4 km) global terrain and landuse
;      6; 30 sec ( ~.9 km) global terrain and landuse
;
NSTTYP=     1,    2,    1,    1,    1,   1,  ;  1 -- ONE WAY NEST, 2 -- TWO WAY NEST
```

Of particular relevance here is the one way nesting configuration. One way nests use fixed lateral boundary conditions; two way nests allow information from the inner nest to propagate outward and affect the outer nest, thereby altering the lateral boundary conditions for the inner nest. For modeling of summertime conditions in southeast Texas, one might suppose that two-way nesting would be preferable, due to the large horizontal scale of the sea breeze response. If the large-scale sea breeze is not properly captured on the larger grids, it may be inhibited on the smaller grids. However, we know of no reason that the large-scale sea breeze would not be simulated properly on the coarser nests.

One-way nests are useful for a particular pragmatic reason: only the nest of interest need be integrated forward in sensitivity tests, thereby saving computer time and limiting the degrees of freedom of the system. Tests of one-way versus two-way nests are described in Section 5.

The first part of the job deck for the basic TERRAIN run is reproduced in Appendix A.

4c: PREGRID and REGRIDDER Configuration Parameters

The model analyses used for the MM5 runs are three-hourly EDAS analyses, available from NCAR. These analyses are designed by NWS to be the best available analyses for mesoscale model initialization. Sea surface temperature information is extracted from the surface temperatures of the EDAS analyses. Such sea surface temperatures must be used with caution. Therefore, a visual inspection of the sea surface temperature fields was performed, and it was found that the sea surface temperatures were realistic all the way to the coastline. Furthermore, the simulated maximum and minimum temperatures at the Galveston NWS station agreed with the model simulation to within half a degree, as discussed in Section 5, suggesting that the sea surface temperatures in the model are producing the proper thermodynamic response in the model atmosphere. Finally, no significant erroneous convection has been found offshore in the model simulations.

The first part of the csh script for the basic PREGRID run is reproduced in Appendix B. The namelist of the 4 km grid run of REGRIDDER is reproduced in Appendix C.

4d: INTERPF Configuration Parameters

The INTERPF preprocessor performs the vertical interpolation to sigma surfaces and the hydrostatic/nonhydrostatic initialization. At this point, the vertical structure of the MM5 run is specified. The basic run includes 43 sigma levels and 42 half-levels, specified as follows:

```
sigma_f_bu     = 1.000,0.990,0.980,0.970,0.960,0.950,     ! full sigma, bottom-up,
                 0.940,0.930,0.920,0.910,0.895,0.880,      ! start with 1.0, end
                 0.865,0.850,0.825,0.800,0.775,0.750,      ! with 0.0
                 0.720,0.690,0.660,0.630,0.600,0.570,
                 0.540,0.510,0.475,0.440,0.405,0.370,
                 0.330,0.290,0.250,0.210,0.175,0.145,
                 0.115,0.090,0.065,0.045,0.025,0.010,
                 0.000
```

The half-sigma levels, on which horizontal winds, temperature, and mixing ratios are computed, are approximately midway between the full sigma levels. The high resolution through the lowest portion of the atmosphere is motivated by previous experience with MM5 simulations of the sea breeze which suggest that at least 15 vertical levels are needed through the depth of the sea breeze in order to properly resolve the sea breeze frontal circulation.

The basic-state definitions of temperature and lapse rate are altered from their default values in order to more closely represent the typical atmospheric state in southeast Texas in summertime.

A complete namelist for the 4 km grid run of INTERPF is reproduced in Appendix D.

4e: MM5 Compilation Options

At compile time, the parameterizations for the MM5 are chosen. The basic MM5 run includes the following parameterizations.

The microphysics scheme is simple ice. This is a fast scheme which tracks cloud water mixing ratio and either rain or snow mixing ratio, depending on the temperature. It is made faster by the use of a look-up table for microphysical parameters. Since accurate simulations of the dynamics of moist convection are not the objective, a relatively simple microphysics scheme is appropriate. If moist convection occurs erroneously in the MM5 simulation, different microphysics schemes may be tested.

The cumulus parameterization is Grell. This scheme, along with Kain-Fritsch, is designed for relatively high horizontal resolution, in the neighborhood of 20-30 km. The Kain-Fritsch scheme has shown wildly varying behavior as the grid resolution decreases to 12 km; the Grell scheme has tended to be much better behaved at such high resolution. Other schemes may be tested if moist convection is a problem on the coarser domains. No cumulus parameterization is used on the 4 km and 1 km grids, where it is assumed that the model can explicitly resolve convective updrafts. The shallow convective scheme is used on all grids.

The PBL parameterization is the MRF scheme. This scheme is a Blackadar-type scheme which incorporates rapid transport throughout the convective boundary layer. In earlier tests with the MRF, Blackadar, and Burk-Thompson schemes, the MRF scheme produced the most realistic diurnal temperature cycle. In an experiment described in Section 5, the MRF scheme is compared to the Gayno-Seaman scheme.

The radiation scheme is the Fast Forward Radiative Transfer scheme. This scheme produced the most realistic diurnal temperature cycle in tests of the real-time MM5 system prior to TexAQS 2000.

The soil scheme is the multi-layer soil model. While the forcing for the sea breeze is likely to be sensitive to the choice of soil model, there is no other viable choice. The simple slab model is crude and is designed for situations in which the evolution of soil temperature is unimportant. The Oregon State University land surface model would have been an interesting test, but the land surface characteristics in EDAS blend gradually toward the ocean rather than transitioning abruptly. As a result, soil moisture, soil temperature, and other parameters are unrealistically specified.

At compile time, the possibility of data assimilation must also be specified.

Excerpts from a configure.user file are given in Appendix E.

4f: MM5 Runtime Options

At runtime, the basic mm5 settings are relatively inconsequential. These settings will become more important later when nudging on the inner nest is attempted. The basic MM5 run includes analysis nudging on the 108 km, 36 km, and 12 km grids, in order that the boundary conditions on the 4 km grid be as accurate as possible.

A sample of the settings for the basic MM5 run is provided in Appendix F.

4g: Hidden MM5 Options

Short of modifying the code itself, there is an additional place for altering MM5: the land surface specification. The basic simulation includes a LANDUSE.TBL file altered from the standard file to reflect the drought in southeast Texas. It is hoped that this modification will not lead to erroneous weather elsewhere where there was no drought, which would then feed back on the innermost simulation.

The distribution of land use types in southeast Texas is shown in Fig. 12. Five land use categories are particularly common: Urban (category 1, Dryland Cropland and Pasture (category 2), Cropland/Grassland Mosaic (category 5), Grassland (category 7), and Evergreen Needleleaf Forest (category 14). The original MM5 settings and their modified versions for the basic run are given in Table 3. Also shown in Table 3 is a further modified version for a test described in Section 5.

TABLE 3: Soil moisture availability in the standard MM5 and in two other model configurations

	Category	Default summertime soil moisture availability	Basic run	Dry test
Urban and Built-Up Land	1	0.1	0.1	0.2
Dryland Cropland and Pasture	2	0.3	0.2	0.1
Cropland/Grassland Mosaic	5	0.25	0.15	0.1
Grassland	7	0.15	0.1	0.1
Evergreen Needleleaf Forest	14	0.3	0.2	0.1

5. Experimental Results

5a: One-Way Versus Two-Way Nesting

This experiment was designed to determine the impact of nesting type on the wind fields within the 4 km nest. The setups for the two model runs are as follows: sep24grid4redux is like the basic run, except analysis nudging is not performed on the 12 km grid, and aug31 is like the basic run, except analysis nudging is not performed on the 12 km grid and all nests are two-way. The two runs are compared by subjective inspection of low-level model variables.

A side note: the unusual title of the first of the above runs is due to a bug discovered in Version 3.4 of MM5 which causes the output time to drift from its preassigned regular interval when run with a high-resolution one-way nest. After the bug was fixed, MM5 was rerun with the original model configuration.

The two model runs are similar. The one-way nest is systematically cooler during the day by about half a degree Fahrenheit and possesses comparable temperatures at night. The temperature differences are greatest, about 2 F, on 8/25 when both models produce convective clouds and precipitation by midday (Figs. 13 and 14). The convection is much more widespread in the one-way nest. In both cases, the convection is also much more widespread than what was observed. As will be discussed below, later simulations do not have this problem.

Wind fields have vector differences on the order of 0-2 m/s, occurring both in small and large patches. Such differences do not appear to be related to systematic differences in convection, the PBL, or other such features. The sea breeze front is essentially indistinguishable between the two simulations (Figs. 15 and 16), suggesting that the development of the frontal circulations is not strongly constrained in the area of interest by the details of the lateral boundary conditions.

We conclude from this experiment that the choice of nesting scheme will cause minor, unpredictable differences in the low-level wind field, with the exception of circumstances which are strongly influenced by convection. Once the diurnal cycle and large-scale winds are simulated to satisfaction, the one-way nest test will be repeated to determine which simulation has the best agreement with observations.

5b: Analysis Nudging

This experiment was designed to determine the appropriateness of analysis nudging on the 12 km domain. The comparison is between the basic run, known as oct25grid4, and the sep24grid4redux run described in Section 5a. Oct25grid4 is nudged toward the EDAS analyses on the 108, 36, and 12 km grids, while sep24grid4redux is nudged toward the EDAS analyses on the 108 and 36 km grids only.

The purpose of analysis nudging in this instance is to constrain the coarse grids to agree closely with observed fields while retaining some degree of dynamical consistency. Analysis nudging represents a tradeoff between two extremes. At one extreme, no analysis nudging is performed, and the model solution is free to evolve according to the initial and boundary conditions and internal dynamics. However, small errors in the initial and boundary conditions and internal dynamics can cause the model solution to

drift substantially from reality after a few days. At the other extreme, a single high-resolution grid may be employed, with boundary conditions taken directly from the analysis. In addition to time resolution issues, this can degrade the model solution because such aspects of the boundary conditions as the PBL structure may be incompatible with the PBL structures which can be simulated by the model.

The analysis nudging experiment investigates a more minor distinction. It is possible that nudging on the 12 km domain may restrict the model's response to the diurnal forcing of the sea breeze if the analyses, which are much coarser, do not properly include the sea breeze. It is also possible that such nudging may interact unfavorably with the MM5's convective parameterization, causing inappropriate development or suppression of convection near the domain boundaries. On the other hand, with no nudging on the 12 km domain the model winds (and other simulated parameters) are more likely to deviate from actual domain-wide weather conditions, as they are being less tightly constrained to agree with the analyses.

Fig. 17 (to be compared with Fig. 13) shows that the 12 km nudging substantially reduces the extent of the erroneous convection on 8/25, limiting it to a few isolated cells along the sea breeze front. These cells fail to develop further, so that by later in the afternoon (not shown) the Houston area is free of convection, in agreement with observations. Less convection develops on other days as well.

A more important difference between the two runs is the improvement in the large-scale winds with 12 km nudging. An example of this may be seen by comparison of Figs. 15 and 18 with the observed fields (Fig. 7). The two model runs differ by several m/s throughout the plotted area. Systematic differences are found both offshore and onshore, and the large-scale wind differences result in differences in the position of the sea breeze front. The observations indicate that neither run is perfect, but the oct25grid4 run (with 12 km nudging) is far superior in its representation of winds over the Gulf of Mexico and the limited inland penetration of the sea breeze toward Houston. This latter aspect of the simulation was identified in Section 2 as a critical process leading to the observed timing and extent of the ozone exceedances on 8/31.

Better large-scale winds are found throughout the simulation period in the oct25grid4 model run. We therefore conclude that nudging to the EDAS analyses should be performed on the 12 km grid.

5c: Evaluation of Diurnal Temperature Cycles

Most work to date has involved evaluation of the modeled diurnal temperatures and winds. As discussed in Section 3, this phase of the work involves adjusting the boundary layer characteristics and inputs of the MM5 so as to allow the MM5 model to reproduce as accurately as possible the diurnal wind and temperature variations on its own.

5c.1) Model runs

The model runs that are compared in this and following subsections are as follows:

oct25grid4: the basic model run, described above

dec6grid4: same as the basic model run, except that an additional sigma level is added adjacent to the ground, at 0.996

dec7grid4: same as dec6grid4, except that the Gayno-Seaman PBL scheme is used instead of the MRF PBL scheme

dec14grid4: same as dec7grid4, except that the soil moisture availability is set to its default values (see Section 4g)

dec16grid4: same as dec14grid4, except that the soil moisture availability is set to dry values (see Section 4g)

These model runs are summarized in Table 4.

TABLE 4: PBL Test Runs

	PBL Scheme	Lowest Sigma Level	Soil Moisture
oct25grid4	MRF	0.99	basic
dec6grid4	MRF	0.996	basic
dec7grid4	Gayno-Seaman	0.996	basic
dec14grid4	Gayno-Seaman	0.996	default
dec16grid4	Gayno-Seaman	0.996	dry

The 0.996 sigma level runs include simulations of most model variables at sigma=0.998, or about 17 m above ground level. The run with the lowest sigma level at 0.99 includes simulations of most model variables at sigma=0.995, or about 42 m above ground level. In the 0.996 sigma level runs, the second lowest full sigma level is at 0.99, identical to the top of the first full sigma level in the basic run. The additional sigma level was added at the request of TNRCC, which needs a lowest sigma level of approximately 40 m for its CAM-x runs. We elected to add a level as described above so as to isolate the effect of higher resolution at the lower boundary without altering the sigma levels above and while preserving a smooth variation in vertical layer separation. Higher resolution in the PBL is potentially beneficial for local PBL schemes such as Gayno-Seaman; the impact on a non-local scheme such as MRF may not be as great.

5c.2) Basic model performance: surface temperatures

The MRF PBL scheme is a Blackadar-type scheme which computes profiles and fluxes of temperature, moisture, and momentum from the ground using similarity theory. Given the MRF PBL assumptions, one can compute, using similarity theory, the meteorological variables at observation height given the land surface characteristics, the skin temperature, and the temperature at the lowest half-sigma level. The standard MM5 output fields now include winds at 10 m above ground level (AGL) and temperature and mixing ratio at 2 m AGL. These heights are standard for NWS surface measurements.

To assess the performance of the model in its prediction of diurnal temperature variations, the maximum and minimum 2 m hourly temperatures from the MM5 runs with the MRF PBL are compared to the maximum and minimum 2 m hourly temperatures from standard National Weather Service (NWS) observations, which are generally taken at a height of 2 m as well. A complete statistical validation of the MM5 should include all available valid observations, but at this stage the objective is to understand the general characteristics of the MM5 simulation. The NWS stations are selected because they are distributed reasonably well about the Houston area and surrounding locations (Fig. 19) and because the measurements are made with consistent instruments at carefully sited locations.

Figure 20 shows the daily observed and simulated maximum and minimum temperatures averaged over the eight NWS stations in the Houston area. The two model runs are much more similar to each other than to the observations. The minimum temperatures from both model runs are too high by 1.5 to 3 C. Maximum temperatures show less bias, but the error tends to grow with time. The model maximum temperatures are slightly too warm early in the episode and are too cold (or, more accurately, not hot enough) later in the episode. Overall, the model runs are deficient in the amplitude of the diurnal cycle, underestimating the warming during the day and the cooling at night. Such an error, if reflected in the atmosphere throughout the PBL, would lead to a weaker than observed diurnal wind cycle, including too weak a sea breeze.

Comparing the two model runs, the maximum temperature simulation is essentially unchanged by the addition of the new lower sigma layer. Minimum temperatures show an improvement, with the warm bias reduced on all days.

The biases vary from station to station. In Table 5, the individual Houston area bias are shown, along with averages of more distant coastal plain stations (Victoria, Palacios, and Beaumont/Port Arthur) and more distant inland stations (College Station, Huntsville, and Lufkin).

TABLE 5: Average daily maximum and minimum temperature biases, 8/25-9/1

Station location	Station ID	oct25grid4 max bias	oct25grid4 min bias	dec6grid4 max bias	dec6grid4 min hi bias
Lake Jackson	LBX	-0.1	3.3	-0.1	2.8
Conroe	CXO	-1.4	3.8	-1.5	3.5
Hobby Airport	HOU	0.8	1.9	0.9	1.5
Spring	DWH	-1.5	3.2	-1.4	2.9
Ellington Field	EFD	-0.5	2.6	-0.5	2.2
Bush Intercontinental	IAH	-1.5	2.8	-1.5	2.4
Galveston	GLS	0.4	0.7	0.3	0.8
Brenham	11R	-2.1	0.4	-2.1	0.0
HOUSTON AREA AVERAGE		**-0.7**	**2.4**	**-0.7**	**2.1**
COASTAL PLAIN AVERAGE		**-1.3**	**2.2**	**-1.3**	**1.8**
INLAND STATION AVERAGE		**-2.0**	**3.1**	**-2.1**	**2.5**

The most accurate simulations are at Galveston. During most of the ozone episode, this particular station received onshore flow from the nearby Gulf of Mexico, so its temperatures largely reflect offshore air temperatures. The small bias at this particular

station implies that the marine boundary layer temperatures (and presumably the underlying sea surface temperatures) are accurate to better than a degree Celsius.

Three stations (Conroe, Spring, and Bush) are similar to each other. All are too cool by about 1.5 C during the day, and are too warm by about 3 C at night. These stations are all located north of Houston, within the Piney Woods (land use category 14), suggesting that the characteristics of this particular category, such as soil moisture, are not specified properly. The inland station average is consistent with this finding. The inland average is also too cool during the day and too warm at night; two of the three inland stations that compose this average are in the Piney Woods as well.

The remaining four stations show no consistent pattern, and because the number of remaining stations is small it is not possible to attribute the biases to the land surface specification with any confidence. Particularly interesting is the differing behavior at Ellington Field and Houston Hobby Airport. Both stations are southeast of downtown Houston and are within 20 km of each other. Yet the error in the amplitude of the diurnal cycle (the difference between the maximum and minimum temperatures) is about 1 C for Hobby and about 3 C for Ellington. Most of this difference is due to model maximum temperatures being over 1 C warmer at Hobby than at Ellington, contrary to observations. It appears that Hobby is under the influence of the urban land use category and therefore experiences the MM5's urban heat island, while Ellington is classified as agricultural and experiences somewhat milder daytime temperatures.

The poor minimum temperature forecasts would be expected to have little direct impact on ozone concentrations, but they are of concern nonetheless. A warm bias in minimum temperatures implies that the nighttime stratification will be too weak. This, in turn, can lead to erroneously high values of nighttime mixing of chemical constituents. Furthermore, the mixing of momentum (winds) could also be too strong, leading to erroneous nighttime transport and affecting the subsequent evolution of winds during the day.

5c.3) PBL Scheme Intercomparison

The model runs dec6grid4 and dec7grid4 are identical except in PBL scheme. A process such as nighttime inversion development can be very sensitive to the PBL parameterization characteristics. There are many differences between the low-level fields in the two runs. For example, the Gayno-Seaman run tends to have more variable winds, a sharper sea breeze front, and a stronger coastal temperature gradient during onshore wind conditions. A comprehensive comparison of the two model runs will be performed at a later date; at this point, we focus on the diurnal temperature cycle.

In order to compare the two runs, it is necessary to examine a model output field other than 2 m temperature, since 2 m temperature fields are not available with the Gayno-Seaman PBL scheme. We also choose four representative stations in the Houston area: HOU, CXO, LBX, and GLS. Since temperature observations are not taken at 17 m height, the simulations cannot be compared directly to observations. However, if one assumes that the errors at 2 m in the dec6grid4 simulation are similar to the errors at the 0.998 sigma half-layer, one can determine whether the dec7grid4 simulation represents an improvement or a degradation.

The comparison of temperatures is given in Table 6. Day-to-day variations in temperature are as much as a degree Celsius, but of variable sign; averaged over the whole episode most differences are essentially zero. The one exception is Galveston (GLS), where the Gayno-Seaman PBL scheme systematically produces a larger diurnal temperature cycle, by about 1 C. This difference is apparently related to the tendency in the Gayno-Seaman simulation to produce stronger temperature gradients near the coastline. In this instance, the MRF PBL is more accurate, in the sense that the amplitude of the diurnal cycle almost exactly matches the observed amplitude. However, the actual distance from GLS to the coastline is poorly resolved at 4 km grid spacing, so it is not known which model run is more accurate given the MM5's coastal configuration.

TABLE 6: dec7grid4 0.998 sigma temperatures minus dec6grid4 0.998 sigma temperatures (C)

	25	**26**	**27**	**28**	**29**	**30**	**31**	**1**	**average**
min hou	-0.4	-0.4	0.0	-0.2	-0.2	0.2	0.3	0.4	**0.0**
max hou	0.3	0.0	0.1	0.1	-0.2	-0.2	-0.4	-0.6	**-0.1**
min cxo	-0.4	-0.2	0.1	-0.5	-0.2	0.1	-0.4	-0.8	**-0.3**
max cxo	-0.5	0.0	-0.4	-0.7	-0.8	0.0	0.2	0.7	**-0.2**
min lbx	0.3	0.3	0.0	-0.2	-0.4	-0.1	0.6	0.3	**0.1**
max lbx	0.9	-0.1	0.8	-1.0	-0.6	0.4	0.2	0.0	**0.1**
min gls	-0.7	-0.4	-0.4	-0.9	-0.4	-0.4	-1.3	-0.2	**-0.6**
max gls	0.3	0.6	0.4	-0.1	0.7	-0.1	0.1	1.2	**0.4**

In summary, the systematic temperature difference between the two PBL schemes seems to be much less important than the difference in the spatial structure of low-level winds and temperatures. The choice of PBL scheme will likely be driven by aspects of the simulation other than the diurnal temperature cycle.

5d: Evaluation of Boundary-Layer Thermodynamic Profiles

One option for fixing the systematic underprediction of maximum temperatures is reduction of the soil moisture content. In order to determine whether such a step is justified by the data, the simulated boundary layer profiles of temperature and moisture are compared to special soundings taken during TexAQS 2000. We use soundings at Wharton (GPS) and Downtown (Airsonde) for this purpose. The Lamarque sounding site was close to the coastline and the PBL is therefore sensitive to simulation errors in wind speed or direction.

In Table 7, the modeled temperature and dewpoint are compared to the observed temperature and dewpoint within the well-mixed PBL. The comparison is performed with respect to the soundings launched every day at about 23 UTC, or late afternoon. Two aspects of the model errors are particularly worthy of note. First, the temperature biases tend to become more negative with time, while the dewpoint biases tend to become more positive. Second, the cool bias at Wharton is accompanied by a moist bias, while the warm bias at Downtown is accompanied by a dry bias. Both of these characteristics imply errors in the partitioning of sensible and latent heat fluxes from the ground, that is, the amount of moisture that is evaporated or evapotranspirated during the day.

TABLE 7: 920 mb to 960 mb average model error in temperature and dewpoint (C), oct25grid4 model run

	8/25	8/26	8/27	8/28	8/29	8/30	8/31	9/1	**average**
Wharton Temp Error	0	0	0	-2	-2	-2	-2	-2	**-1.3**
Wharton Dewp Error	-2	0	-2	2	2	4	2	-1	**0.6**
Downtown Temp Error	2	2	0	-2	1	0	0		**0.4**
Downtown Dewp Error	-4	-5	-2	3	-3	3	2		**-0.9**

The temperature and dewpoint trends are consistent with the weather during and immediately preceding the ozone episode. On 8/23 and 8/24, widespread showers were found in the Houston metropolitan area. The precipitation from these showers, generally much less than an inch, fell on ground which was very dry from several months of drought. Throughout the ozone episode, 8/25-9/1, no precipitation fell. The surface moisture present at the beginning of the episode should have rapidly evaporated, leaving very dry conditions near the end of the episode. With time, then, the soil moisture would decrease, causing (all else being equal) a gradual increase in temperature and decrease in dewpoint.

The model simulation essentially tests this idea by holding soil moisture constant while letting the rest of the atmospheric conditions vary in a realistic manner. The result is model that gradually becomes wetter and cooler than the real atmosphere, as the water available for evaporation into the real atmosphere gradually vanishes.

If a systematic difference in temperature from one location to another is to be explained by variations in soil moisture, the warmer location must also be the drier one. This pattern is followed with the Wharton and Downtown sites: the model errors are consistent with too much soil moisture at Wharton and too little soil moisture at Downtown. Perhaps the more heavily populated urban areas are associated with more evaporation because of extensive irrigation of lawns and gardens.

To determine the magnitude of the impact of soil moisture on the MM5 simulations, we compare the dec7grid4 run with a run with more moisture (dec14grid4) and a run with less moisture (dec16grid4). Results are consistent from day to day; the soundings from late afternoon 8/30 are shown in Fig. 21. The specified variations in soil moisture availability produce temperature changes on the order of 2 C and dewpoint changes on the order of 3 C. When moisture availability increases, the temperature falls and the dewpoint rises.

Also plotted in Fig. 21 is the corresponding sounding from the basic run. The basic run used intermediate soil moisture values, yet the PBL is comparable to the driest Gayno-Seaman run. Also noteworthy, and possibly related, is the larger depth of the mixed layer in the basic run with the MRF PBL. Potential temperature and mixing ratio are essentially uniform up to 800 mb in the MRF PBL, whereas the Gayno-Seaman well-mixed layer extends only up to 900 mb. Plots of hourly temperatures show that the Gayno-Seaman PBL attains its highest surface temperatures about three hours before the MRF PBL; based on the sounding data, it appears that the Gayno-Seaman PBL is collapsing prematurely.

These runs suggest that it is appropriate to modify the soil moisture to improve the boundary layer characteristics. This procedure must not be done in isolation; for example, work by R. Zamora of NOAA/ETL implies that radiative errors also contribute

to the PBL thermodynamic errors. These two sources of error are not easily distinguished by inspection of thermodynamic profiles, since both a dry ground and enhanced incoming radiation should produce a deeper, warmer, and drier PBL.

5e: Evaluation of Diurnal Wind Variations

Investigation of the model-simulated variation in the wind over the course of the day has focused on nighttime winds during the second half of the episode. At least some of the apparently poor agreement between the model simulations and the profiler data appears to be related to the modification of the nighttime winds by a convective outflow which is erroneously simulated to pass across the Houston area overnight on August 31-September 1. Presentation of results at this stage would be premature.

6. Conclusions and Future Work

Conditions leading up to the August 25- September 1, 2000, ozone episode were much drier than normal, leading to unusually high temperatures during the latter half of the episode. One-hour ozone exceedances occurred on five of the seven days of the episode, with peak hourly averages of 199 PPB on 8/30 and 194 PPB on 8/25.

The first half of the episode (Regime I), through August 29, was characterized by large-scale onshore flow and stagnant or near-stagnant conditions during mid-morning. By afternoon, winds had picked up from the southeast, and would rotate clockwise and develop a westerly component after midnight. On a hodograph, this diurnal wind variation traces a nearly perfect circle, and profiler data indicates that little wind shear is present. The pattern of wind variation is generally consistent with linear theory of the sea breeze near 30 N latitude.

The second half of the episode (Regime II), beginning August 30, was characterized by shore-parallel or offshore large-scale flow and stagnant or near-stagnant conditions during mid-afternoon. Pollutants were frequently carried southeast away from the city to Galveston Bay, only to return behind the bay breeze later in the afternoon. At night, a strong (7-13 m/s) low-level jet developed a few hundred meters above the ground, with winds decreasing to near zero by an altitude of 1 km. This jet forms in the classic nocturnal low-level environment, with adverse thermal wind shear, and is enhanced by the diurnally-varying sea breeze forcing. Accurate simulation of this jet should require accurate simulation of the vertical mixing of momentum and the decoupling of winds aloft from the PBL.

The strong diurnal signal demands a modeling approach that seeks to configure the model to simulate the diurnal wind and temperature cycle on its own, with as little nudging as possible. Critical aspects of the model configuration include the soil moisture and other land surface characteristics, the PBL parameterization, the vertical grid structure, and the incoming longwave and shortwave radiation. Model validation procedures should begin with phenomenological and focused statistical measures of performance with regard to the diurnal cycle of winds and temperatures as a function of height, and evolve into comprehensive statistical measures of model performance.

Tests of the nesting configuration indicate that analysis nudging should take place on the 12 km grid as well as the 36 km and 108 km grids. The model run with 12 km nudging (oct25grid4, also known as the basic run), produces realistic large-scale winds, sea breeze evolution, and precipitation coverage on most days of the episode. This model run is most deficient on the final two days of the episode, when too-widespread convection influences the Houston area winds and PBL structure.

Forecasts of maximum and minimum temperatures are strongly biased in the basic model configuration, with maximum temperatures too low in the model (by about 1 C) and minimum temperatures too high (by about 2 C). This overall model bias is improved slightly by the addition of new, thin lowest model layer. The MRF and Gayno-Seaman PBL schemes produce similar diurnal temperature cycles with the model configuration employed here, but other boundary layer characteristics are strongly altered by the choice of parameterization and must be further investigated.

Preliminary results suggest that the MRF scheme produces superior daytime boundary layer structure. Of all the model runs so far, the best seems to be the dec6grid4

run, with the MRF PBL scheme and the extra sigma layer near the surface. Anyone wishing to examine the MM5 model performance in more detail is encouraged to work with the dec6grid4 run.

Future work will involve establishment of an optimal land surface configuration using existing land surface categories, and extensive investigation and testing of the model simulations of nighttime Regime II winds. Once a satisfactory diurnal cycle is obtained (or prior to that, if time becomes short), profiler and Doppler lidar data will be assimilated in a coarse fashion to help constrain the large-scale winds.

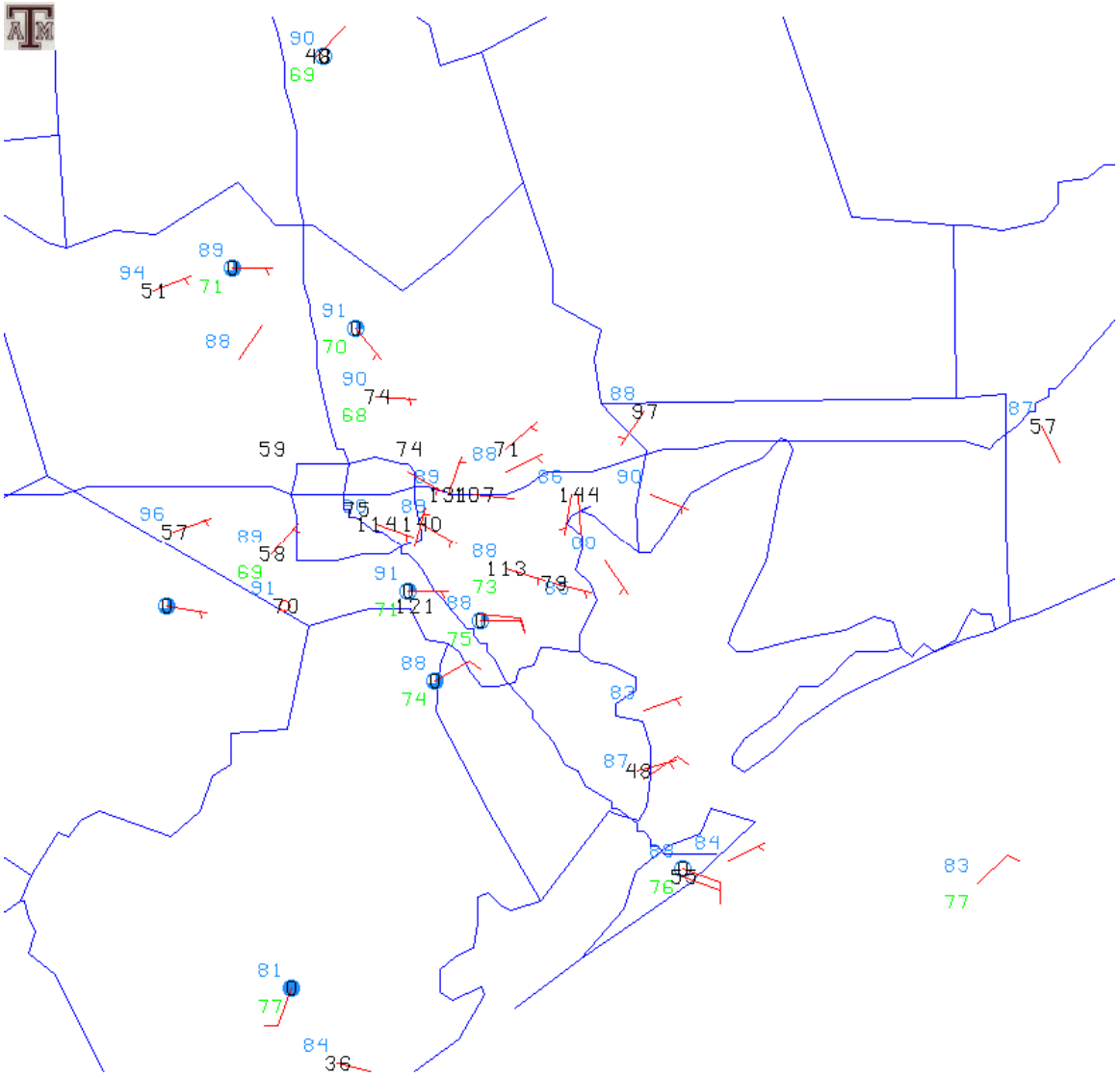

FIGURE 1: Surface map, 1800 UTC (1300 CDT) August 25, 2000. Winds are red, with a short barb equal to 5 knots and a long barb equal to ten knots. Five-minute ozone values are in black (PPB), temperatures are in blue (F), and dewpoints are in green (F).

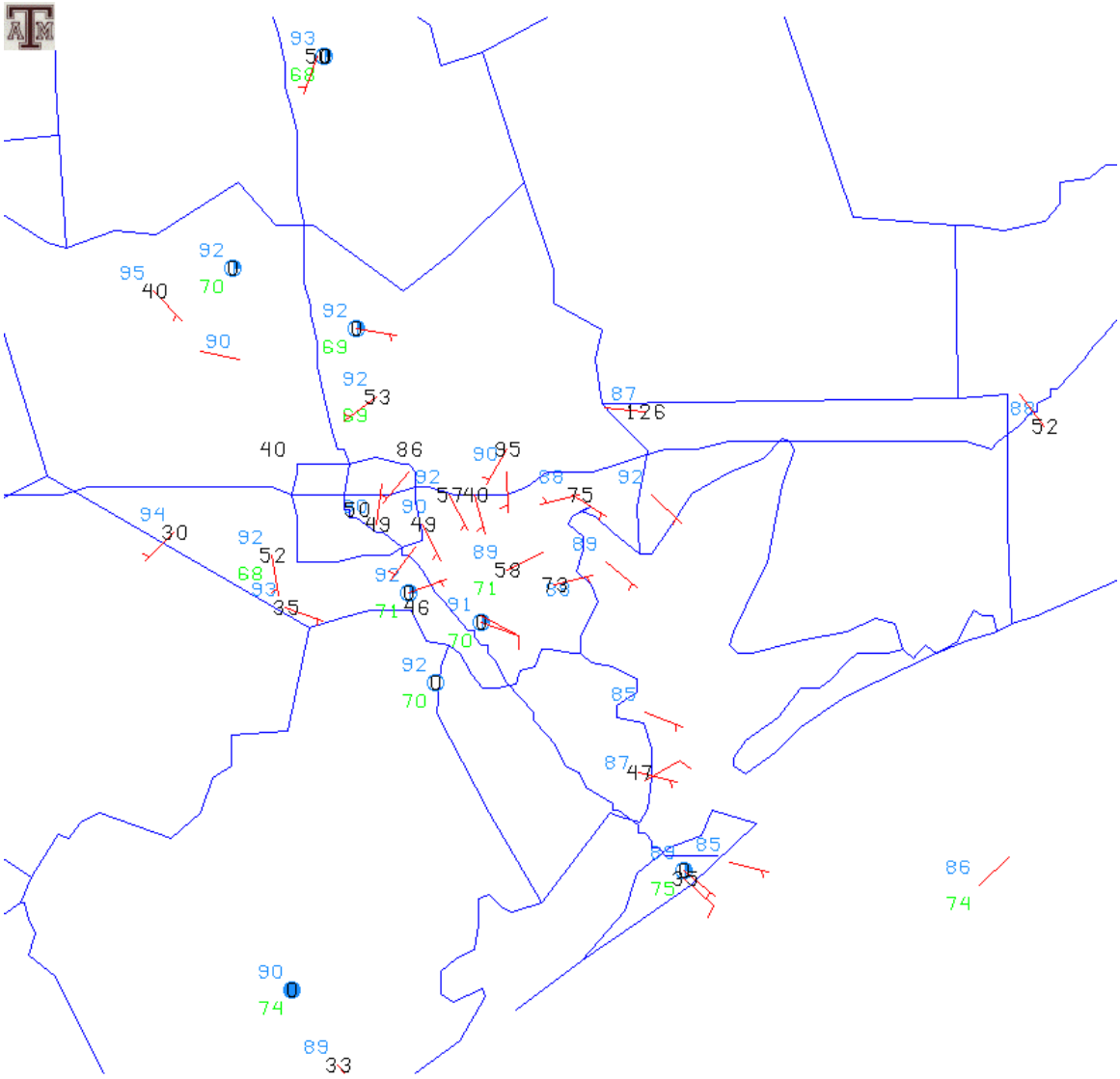

FIGURE 2: Surface map, 1800 UTC August 26, 2000. Plotting convention as in Fig. 1.

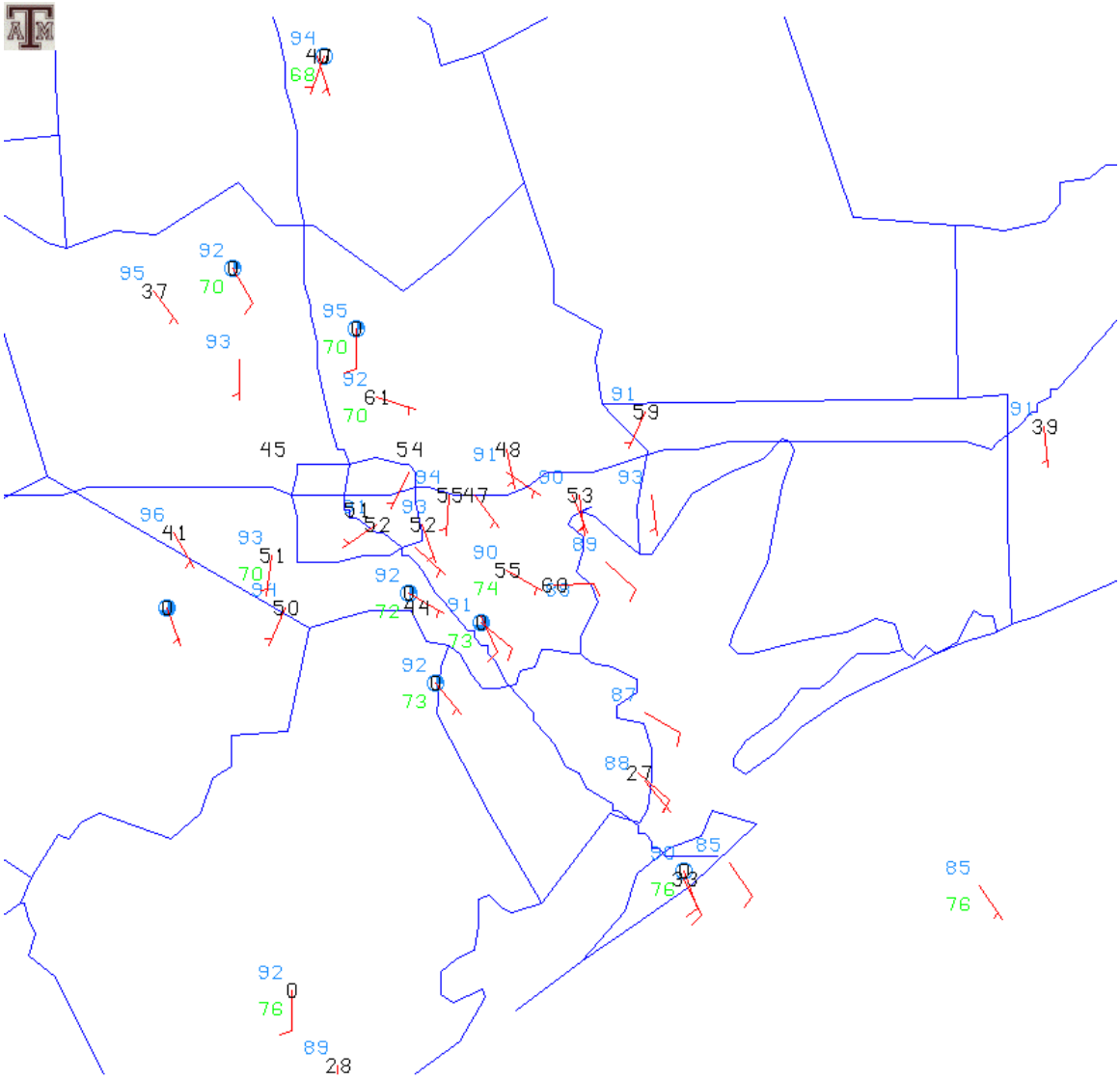

FIGURE 3: Surface map, 1800 UTC August 27, 2000. Plotting convention as in Fig. 1.

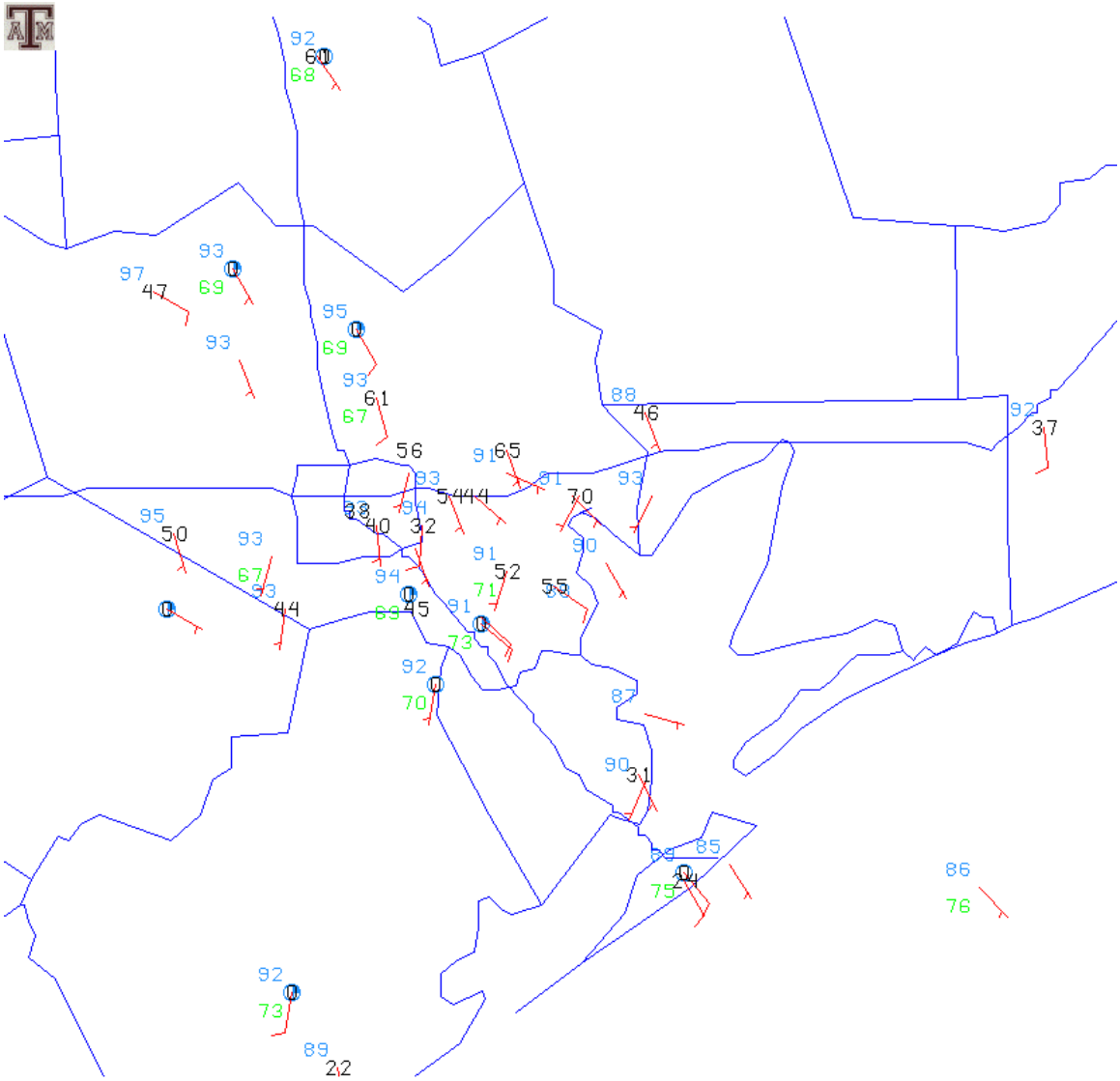

FIGURE 4: Surface map, 1800 UTC August 28, 2000. Plotting convention as in Fig. 1.

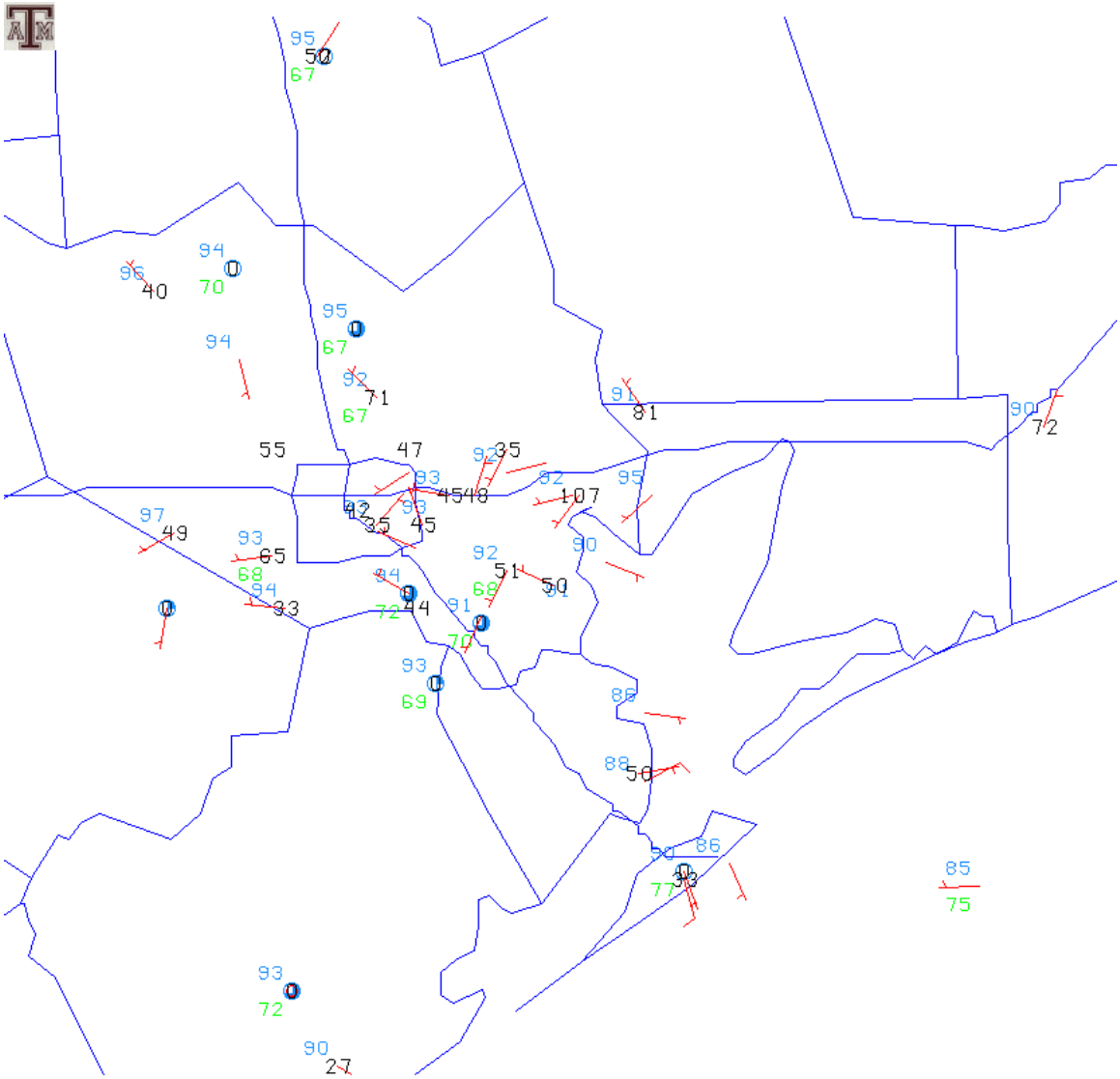

FIGURE 5: Surface map, 1800 UTC August 29, 2000. Plotting convention as in Fig. 1.

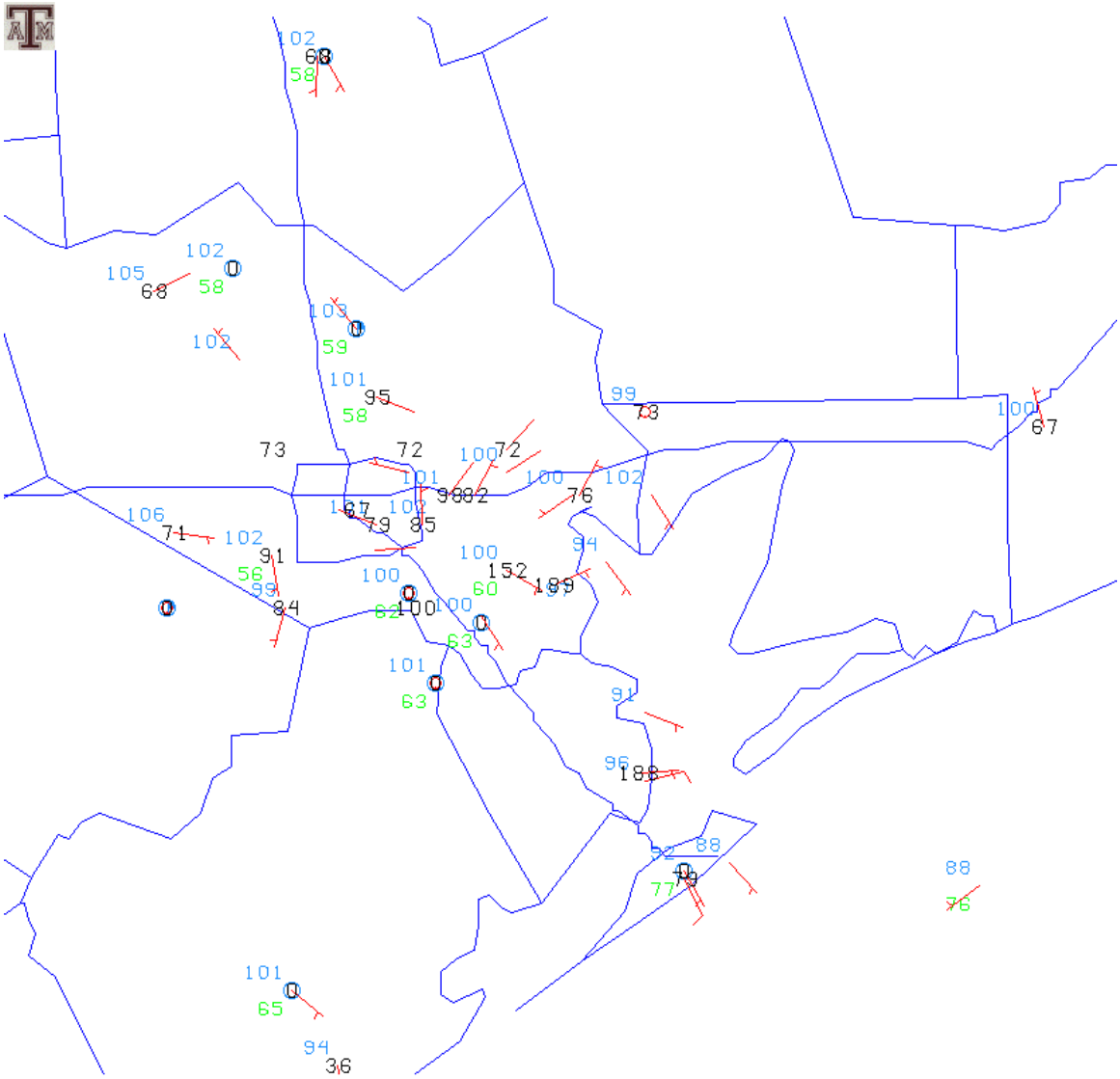

FIGURE 6: Surface map, 2100 UTC August 30, 2000. Plotting convention as in Fig. 1.

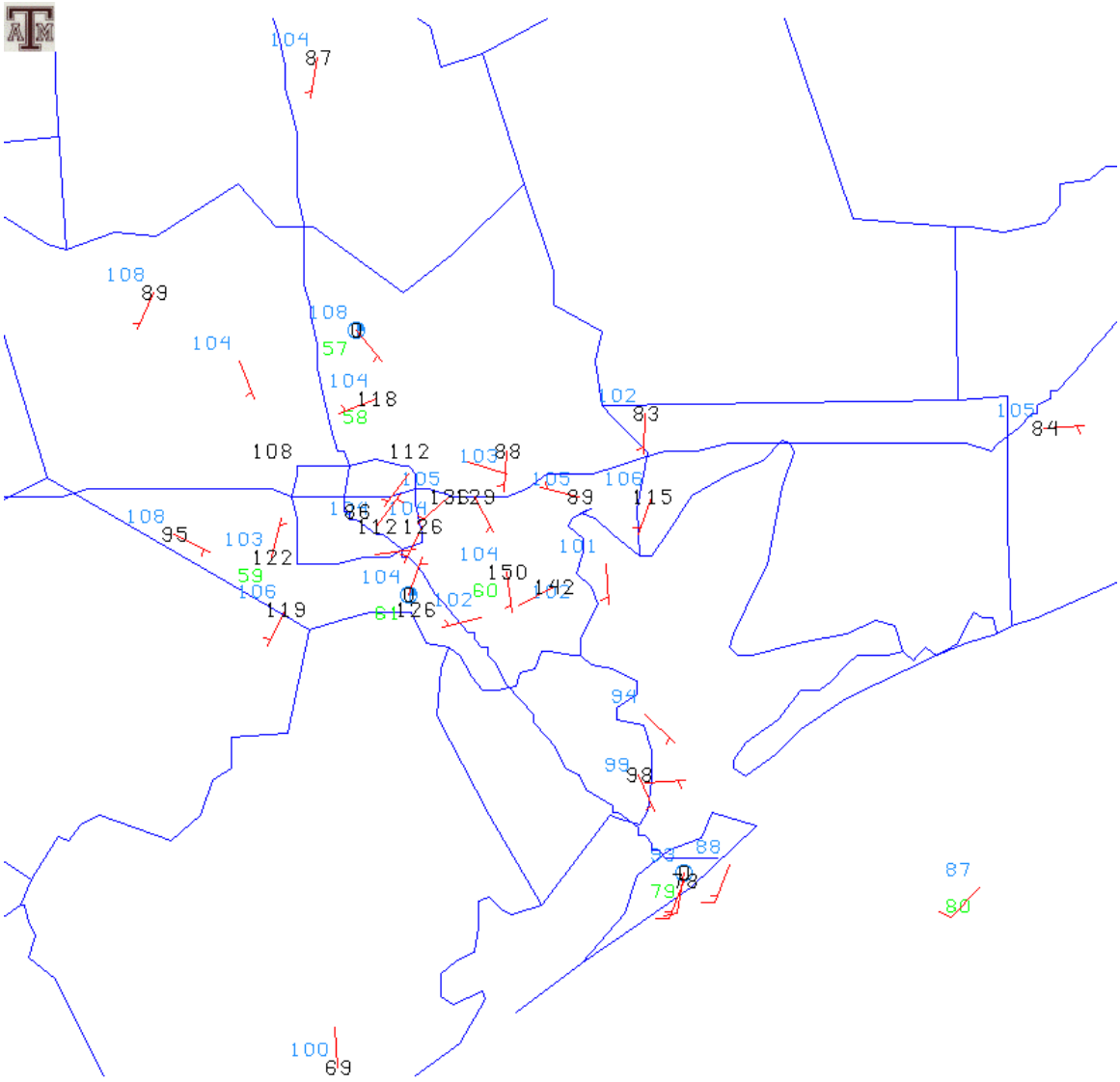

FIGURE 7: Surface map, 2100 UTC August 31, 2000. Plotting convention as in Fig. 1.

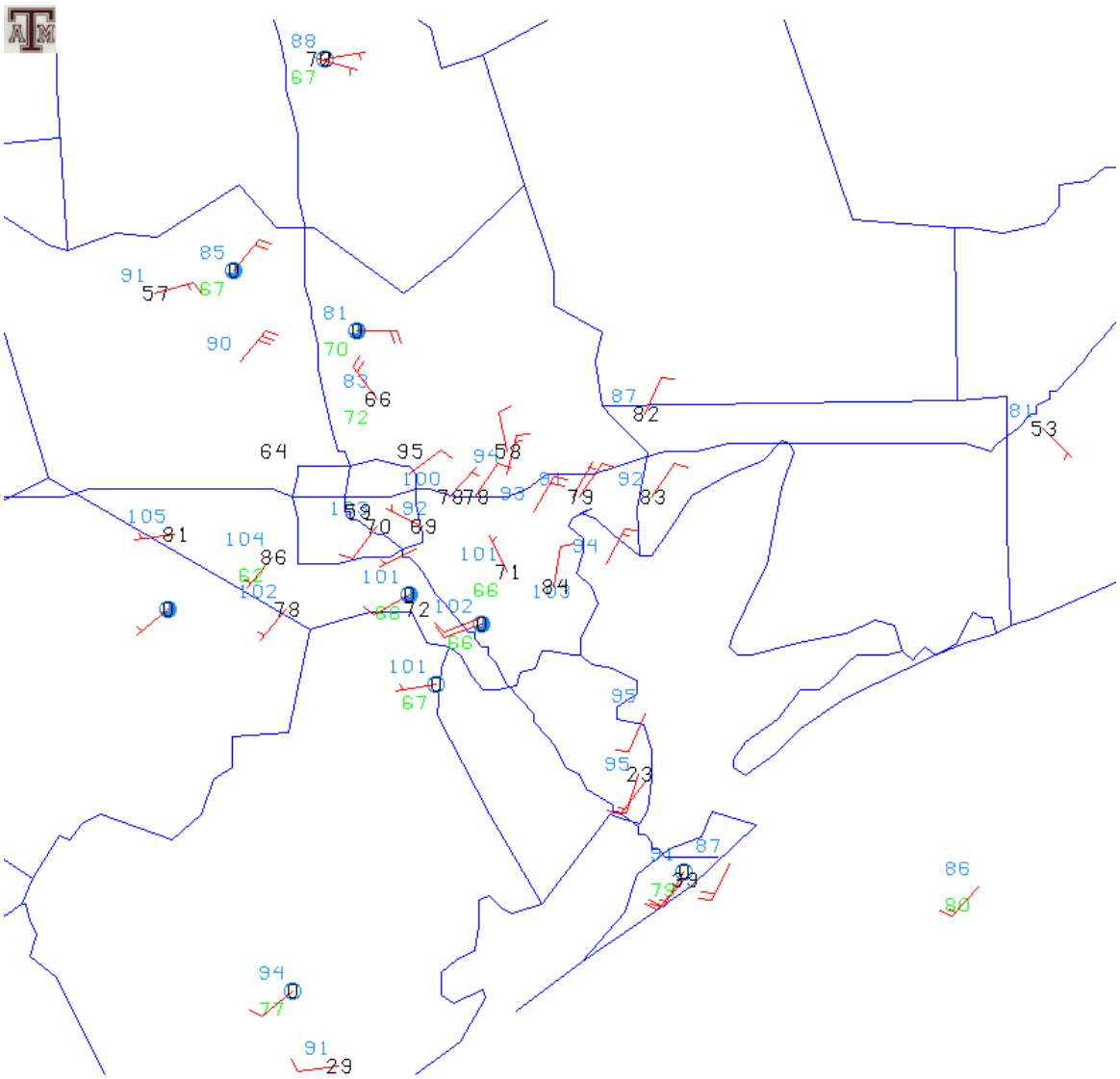

FIGURE 8: Surface map, 2300 UTC September 1, 2000. Plotting convention as in Fig. 1.

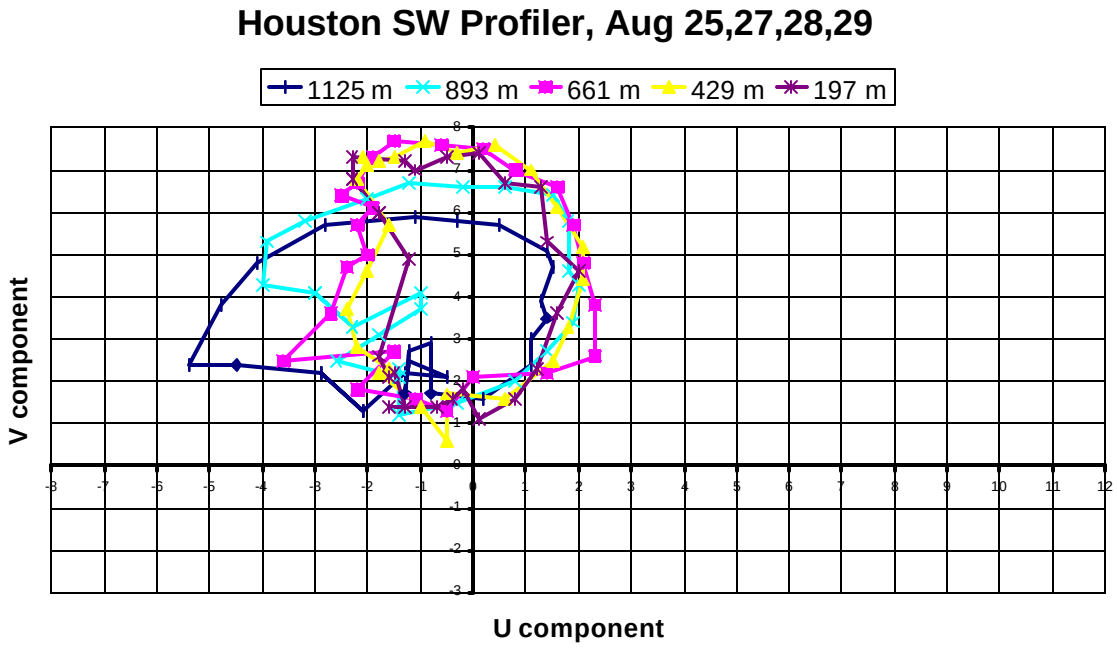

FIGURE 9: Time hodograph showing composite diurnal wind cycle, Houston Southwest Airport profiler. The V component of wind is oriented north/south; each grid box represents 1 m/s. Winds are averaged for each hour on August 25, 27, 28, and 29, 2000. The altitude of each time hodograph is indicated by the legend. The wind at a given level and hour can be represented as a vector that begins at the origin and ends at the appropriate point on the curve. The strongest southerly winds occur between 9 PM and Midnight CST. The trace of the mean winds rotates clockwise on the hodograph so that early morning winds are from the southwest and late morning winds are light. Data provided by NOAA/ETL.

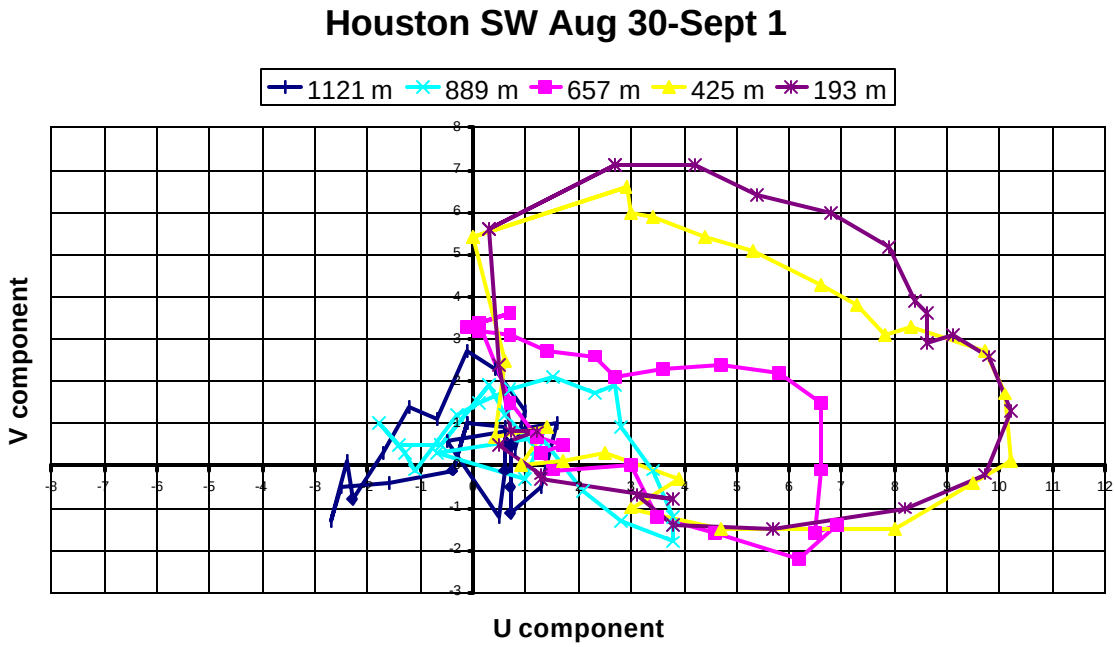

FIGURE 10: Time hodograph from the Houston Southwest Airport profiler, composited for each hour on August 30, 31, and Sept. 1. The strongest winds are from the west and occur around sunrise at low levels in the atmosphere. During the morning the low-level winds rapidly weaken, and the weakest winds are found in early to midafternoon. The strong diurnal wind cycle decreases in amplitude to nearly zero at a height of 1 km. Data provided by NOAA/ETL.

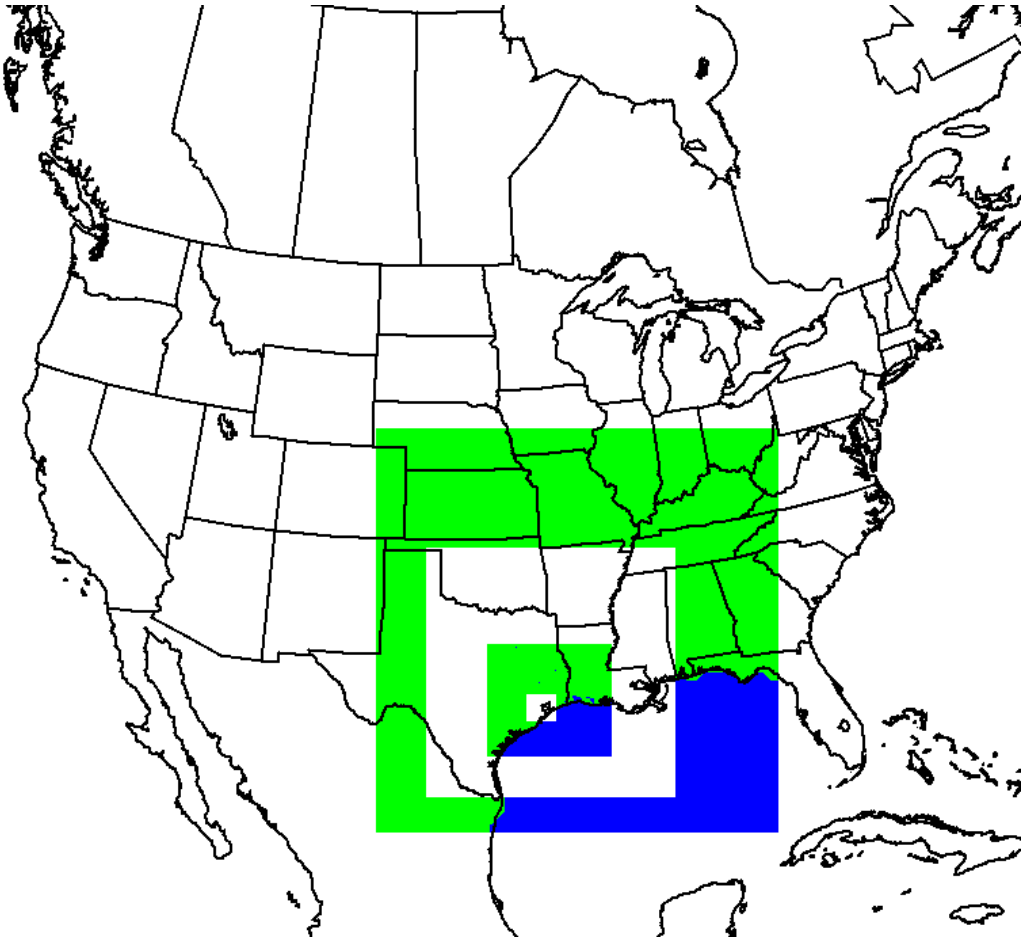

FIGURE 11: MM5 nested grid configuration, August ozone episode. The 108 km grid occupies the entire area of the figure. Nested within that grid are a 36 km grid, a 12 km grid, a 4 km grid, and an experimental 1 km grid.

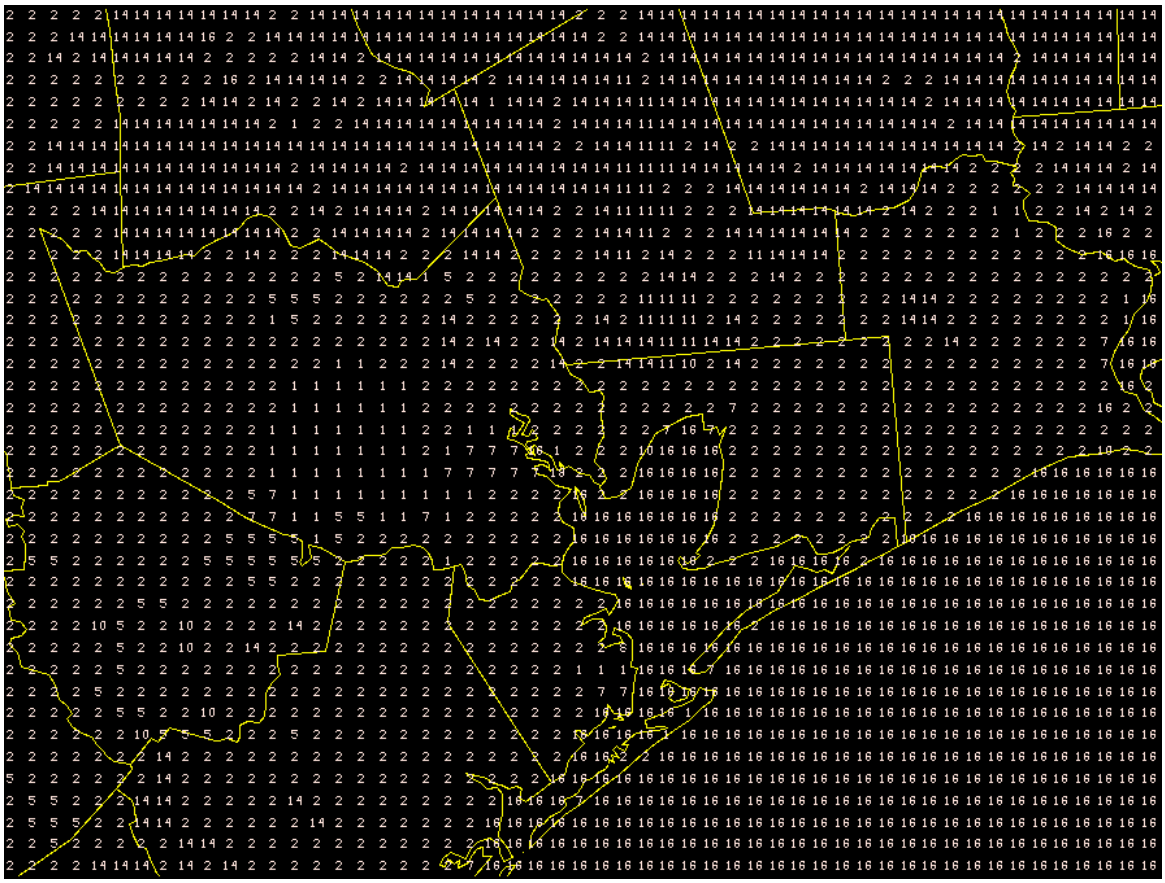

FIGURE 12: Land use categories for the MM5, shown on a subset of the 4 km grid. See text for description.

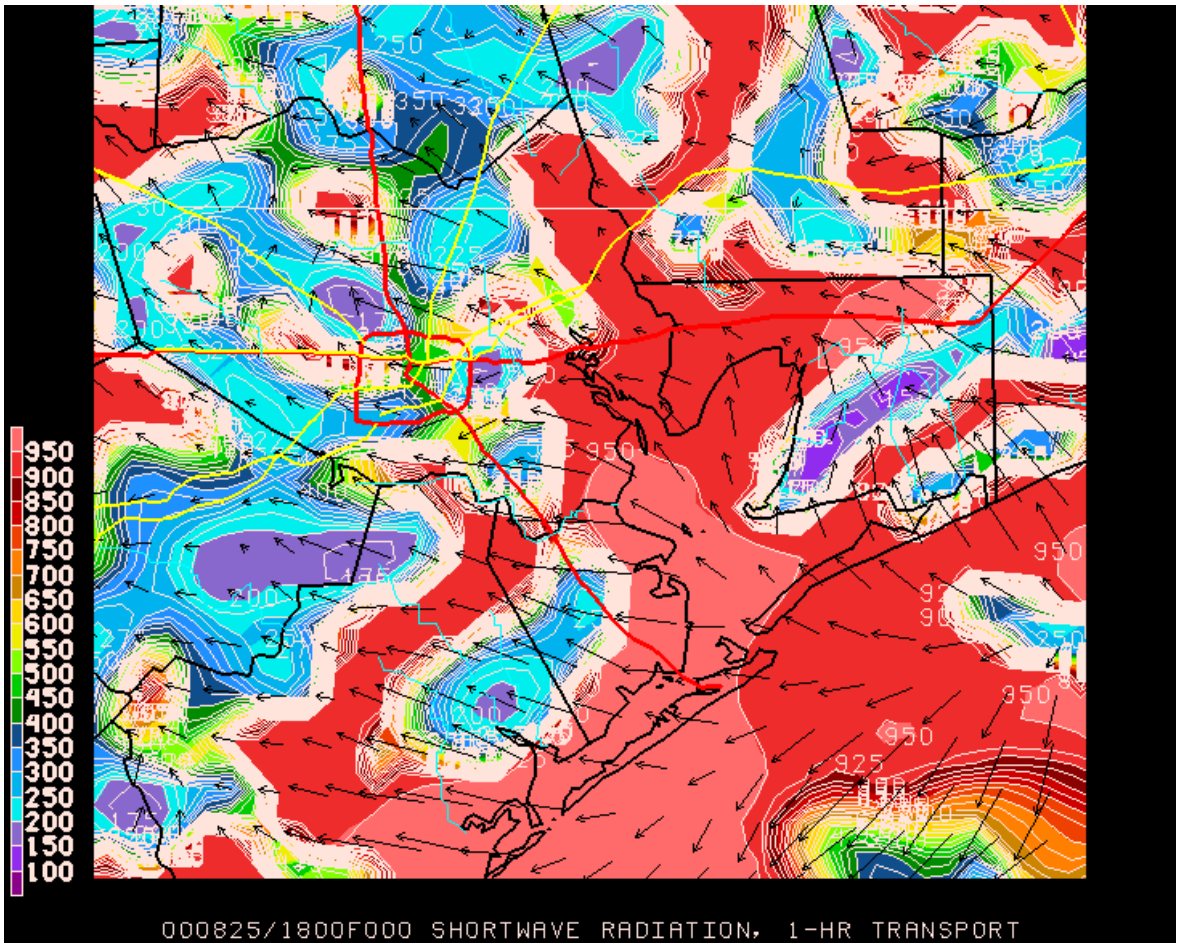

FIGURE 13: Ten-meter winds (scaled to represent one-hour transport) and short wave radiation reaching the surface (W/m**2, low values imply clouds), 18 UTC August 25, 2000, from the sept24grid4redux simulation.

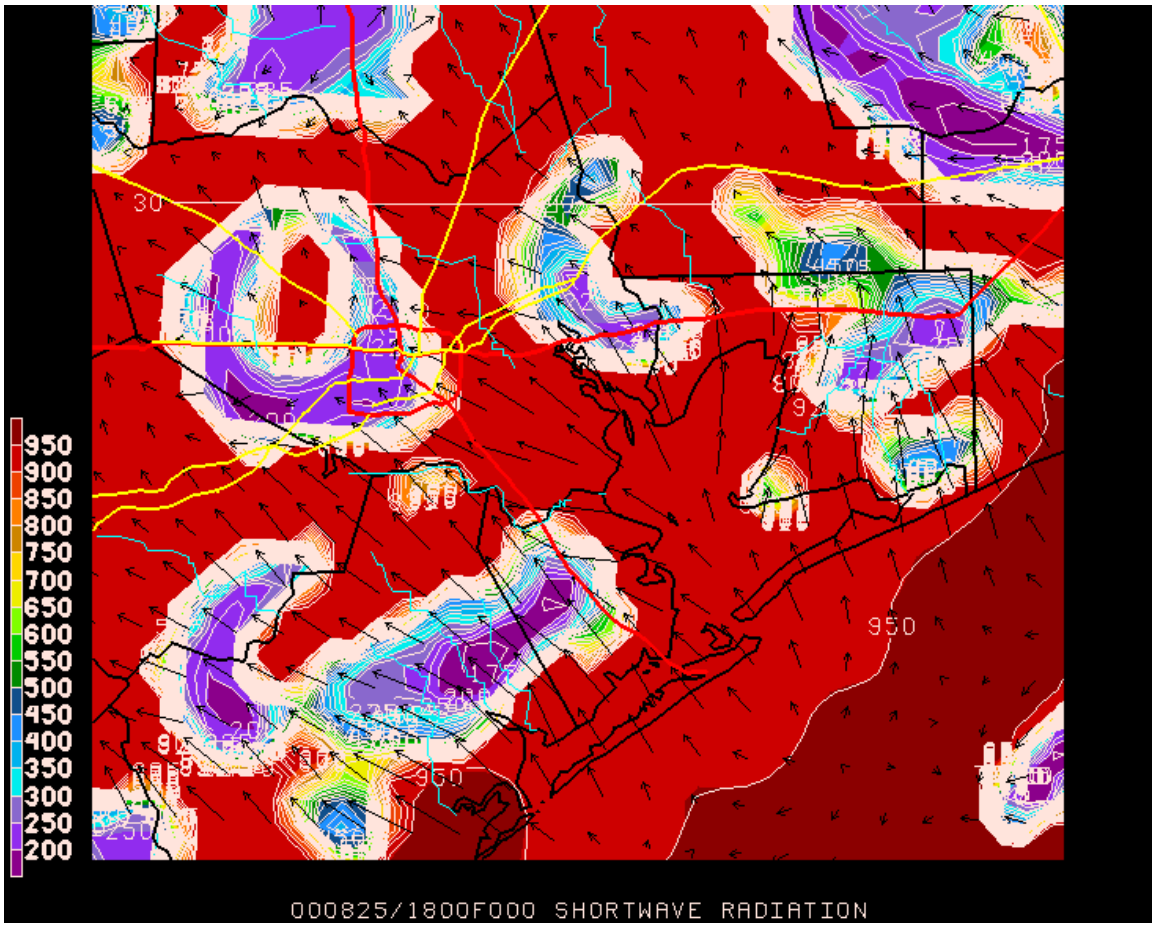

FIGURE 14: Winds and shortwave radiation, 18 UTC August 25, 2000, as in Fig. 13, except from the aug31 simulation.

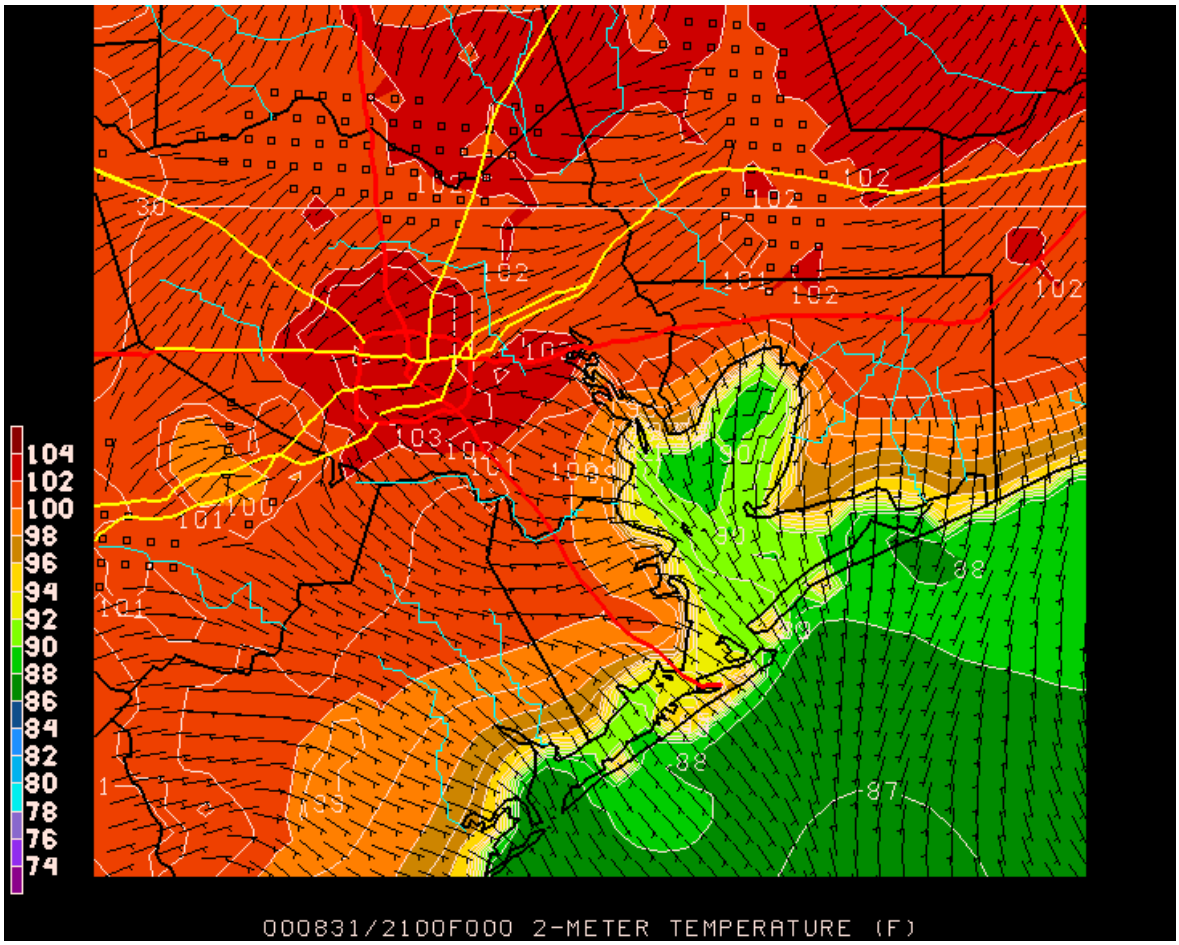

FIGURE 15: Temperatures (F; 2 m above ground) and surface winds (10 m above ground), 21 UTC August 31, 2000, from the sept24grid4redux simulation. Wind plotting convention as in Figs. 1-8.

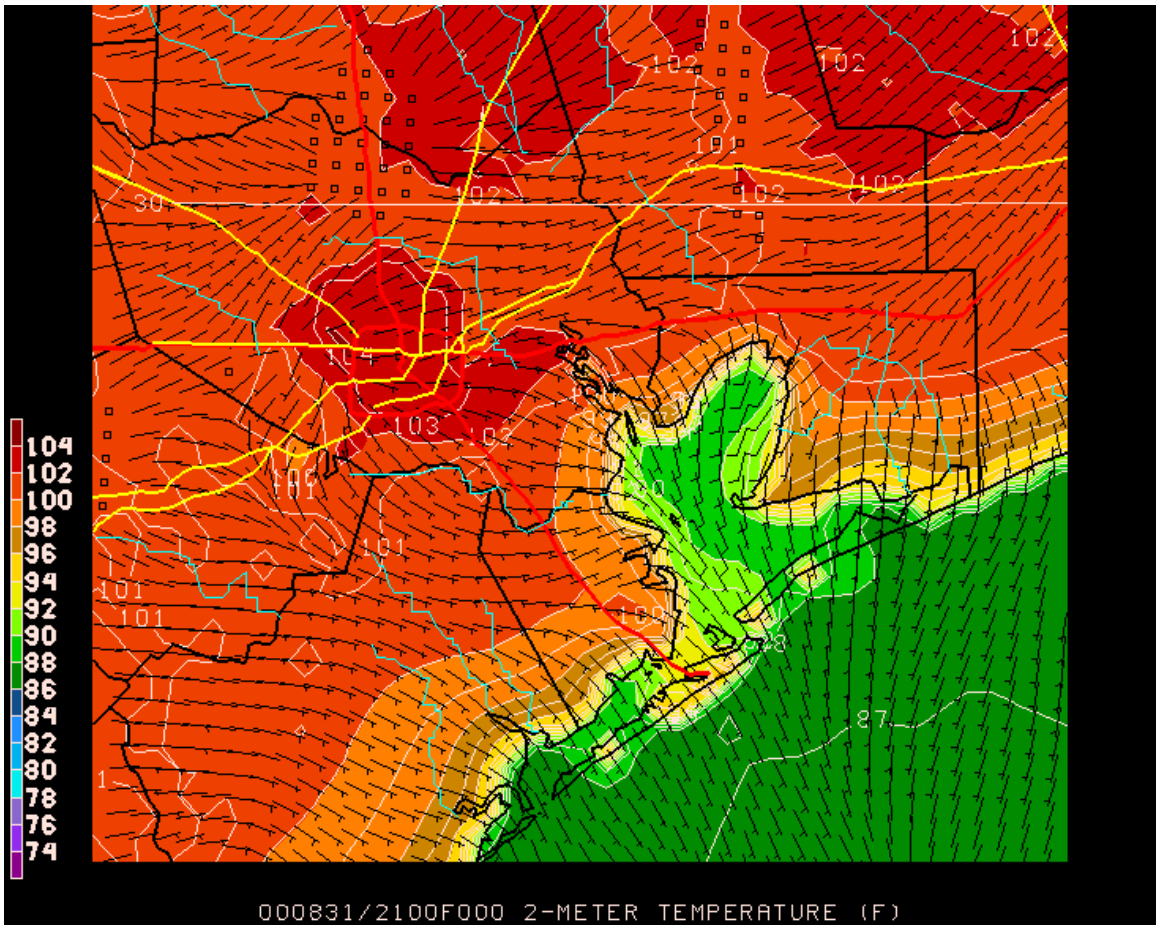

FIGURE 16: Temperatures and winds, 21 UTC August 31, 2000, as in Fig. 15, but from the aug31 simulation.

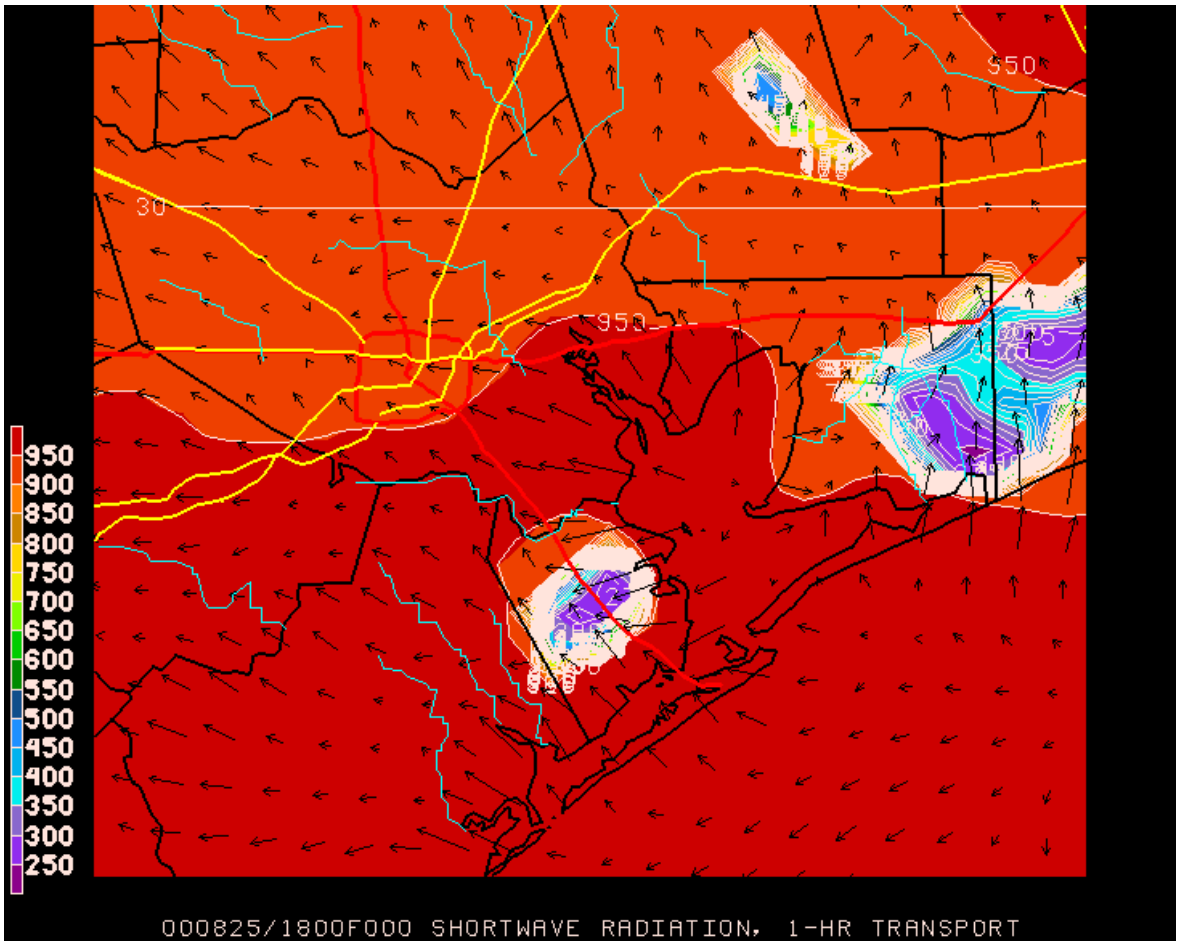

FIGURE 17: Incoming shortwave radiation and winds, 18 UTC August 25, 2000, as in Figs. 13 and 14 except from the oct25grid4 simulation.

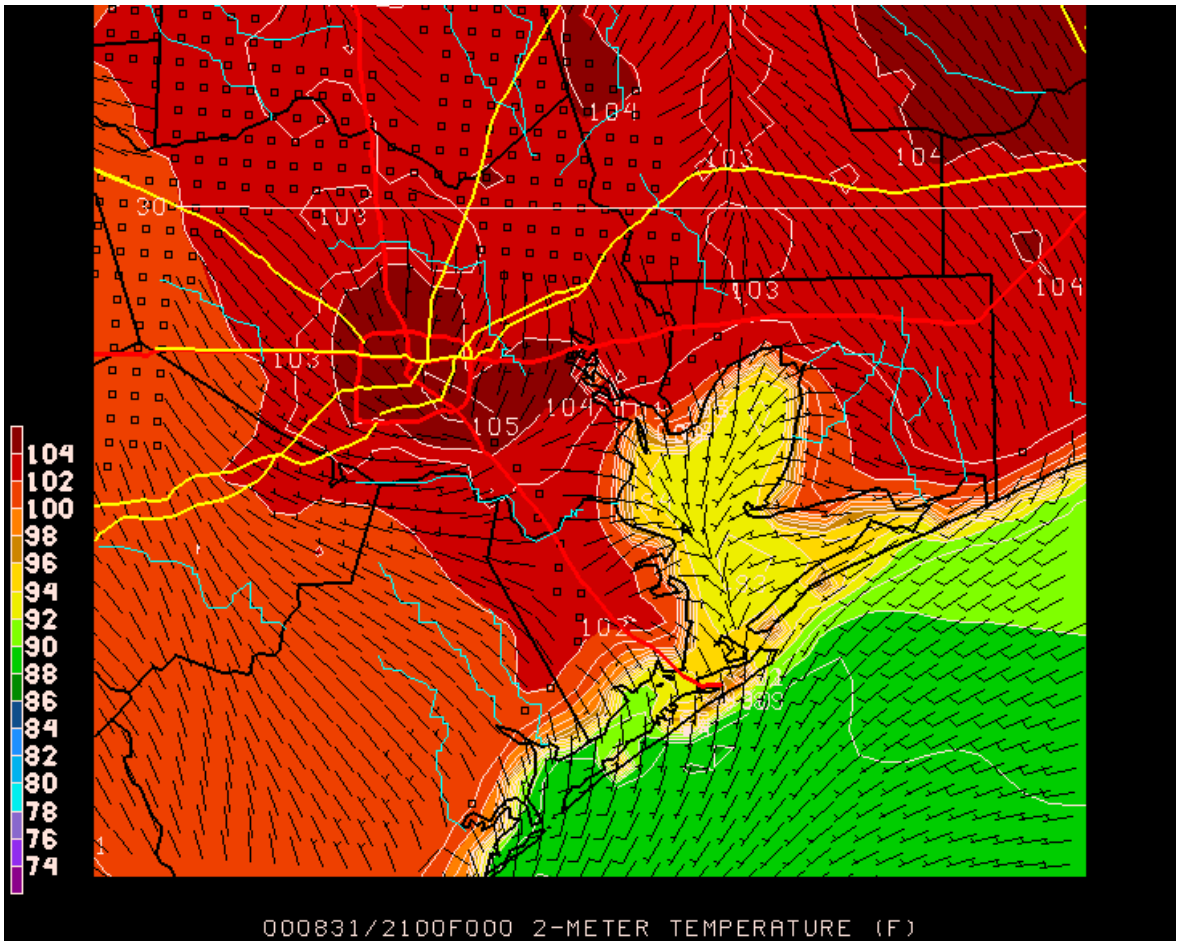

FIGURE 18: Surface temperatures and winds, 21 UTC August 31, 2000, as in Figs. 15-16 but from the oct25grid4 simulation.

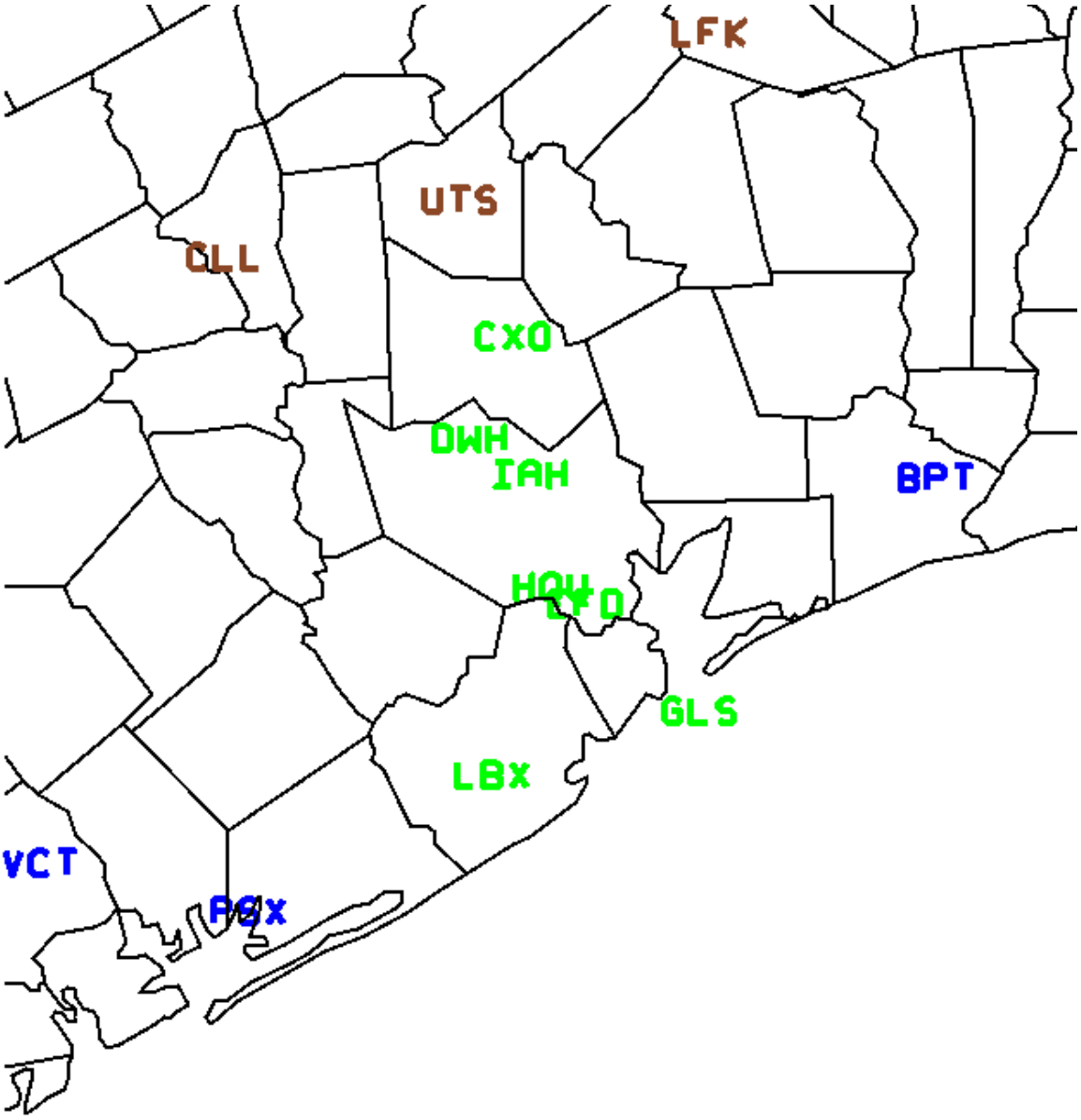

FIGURE 19: Locations of National Weather Service regular observing stations in Houston and surrounding areas. Green stations are treated collectively as Houston area stations (not pictured: 11R, located west of DWH and south of CLL); blue stations are coastal plain stations, and brown stations are inland stations.

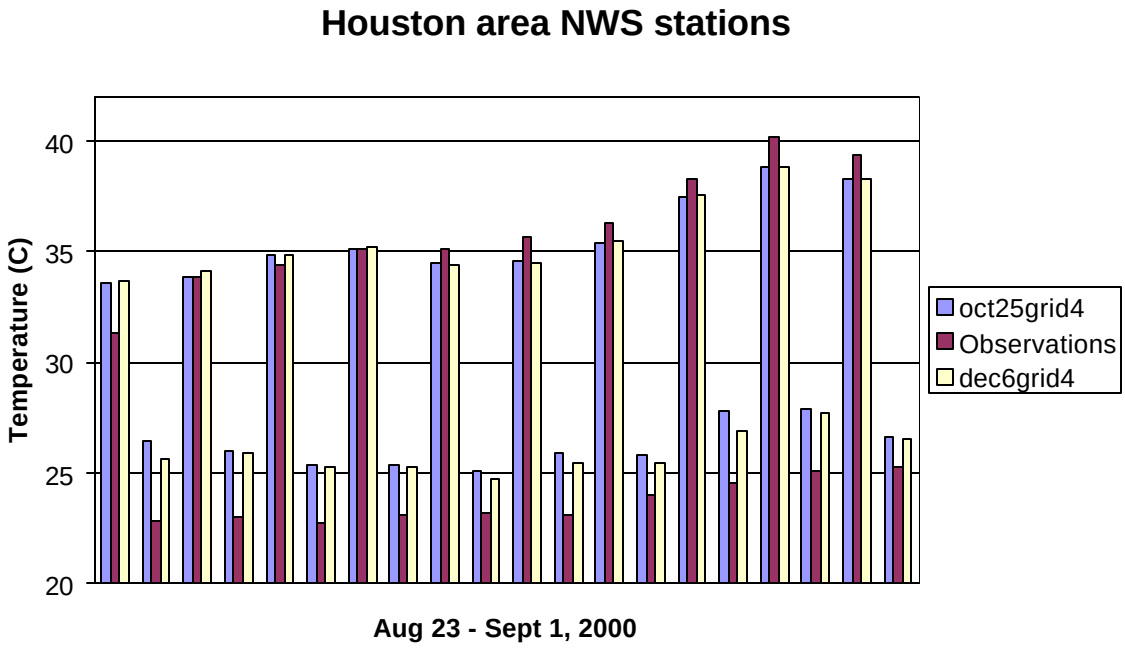

FIGURE 20: Comparison of hourly maximum and minimum temperatures averaged from eight station locations in the Houston area with two model forecasts. Successive groupings of data, from left to right, are maximum temperatures, August 23, 2000, minimum temperatures, August 24, maximum temperatures, August 24, etc.

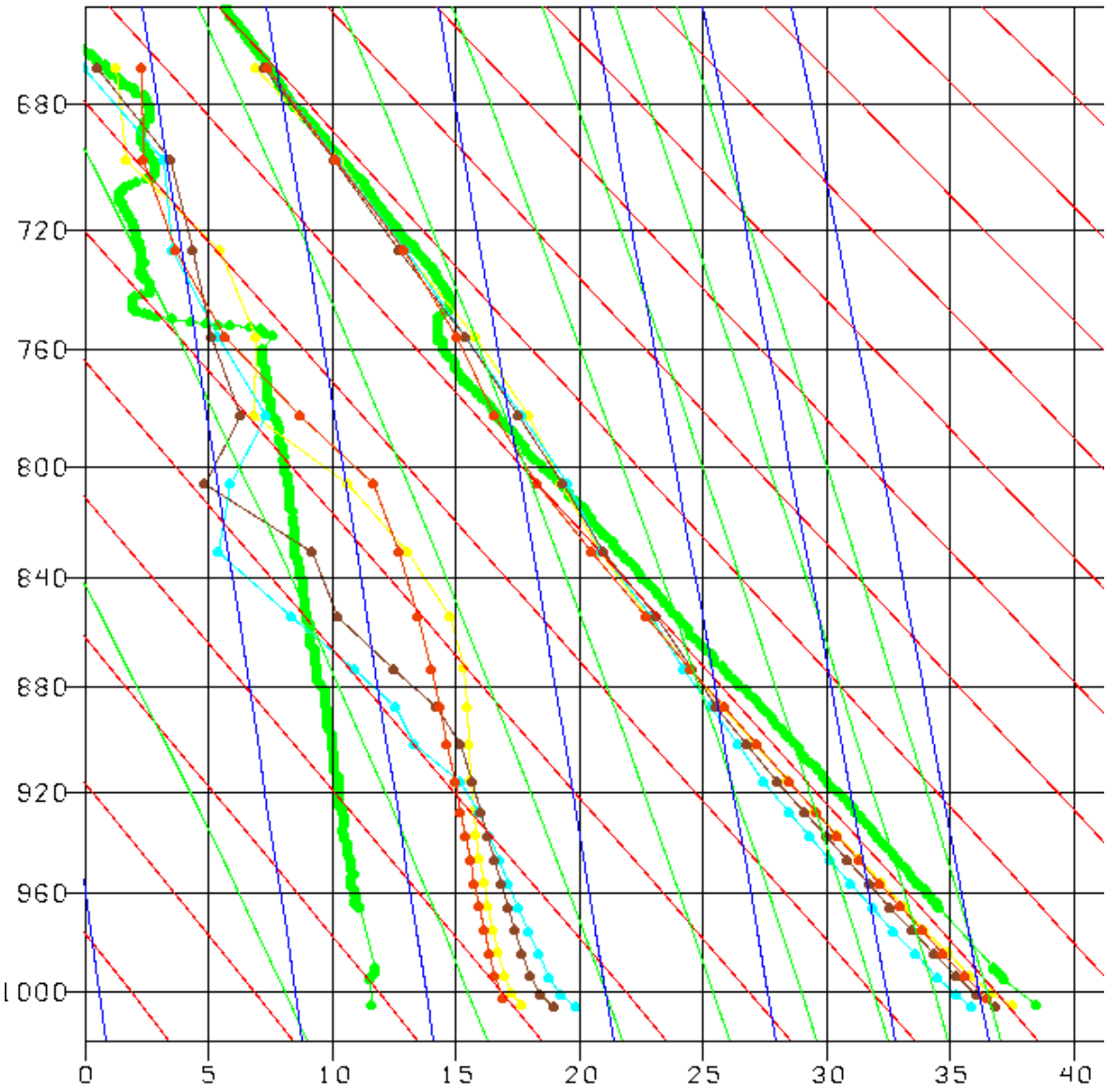

FIGURE 21: Stuve diagram, 23 UTC August 30, 2000, Wharton Power Plant rawinsonde launch site. Green: rawinsonde observations of dewpoint and temperature (Celsius). Light blue: dec14grid4 simulation (default soil moisture). Brown: dec7grid4 simulation (basic soil moisture). Yellow: dec16grid4 simulation (dry soil moisture). Red: oct25grid4 simulation (basic soil moisture, MRF PBL). Background lines are, clockwise from horizontal, pressure (mb, black), potential temperature (red), equivalent potential temperature (green), saturation mixing ratio (blue), and temperature (C, black).

APPENDIX A: Basic `terrain.deck`

This job deck is reproduced from `/met/ngammon/analyses/oc1501/terrain.deck`.

```
#!/bin/csh -f
# terrain.csh
#
set echo
#
#   Set this if you would like to ftp terrain data
#
#set ftpdata = true
set ftpdata = false
#
#   Set the following for ftp'ing 30 sec elevation data from USGS ftp site
#
#set Where30sTer = ftp
set Where30sTer = /met/bcd/TERRAIN/Data
if ( $Where30sTer == ftp) then
#
#    Use this if you are ftping from other places
#
#    set users = Others
#
#    Use this if you are ftping from MMM/NCAR
#
     set users = MMM
else
     set users =
endif
#
# ---------------------------------------------------------------
#          1. Set up parameter statements
# ---------------------------------------------------------------
#
cat > src/parame.incl.tmp << EOF
C      IIMX,JJMX are the maximum size of the domains, NSIZE = IIMX*JJMX
       PARAMETER (IIMX = 136, JJMX = 151, NSIZE = IIMX*JJMX)
EOF
cat > src/paramed.incl.tmp << EOF
C      ITRH,JTRH are the maximum size of the terrain data.
C      NOBT = ITRH*JTRH, here assuming
C      ITRH= 270 ( 45 deg. in north-south direction, 10 min. resolution)
C      JTRH= 450 ( 75 deg. in north-south direction, 10 min. resolution)
C  NOTE:
C      IF USING GLOBAL 30SEC ELEVATION DATASET FROM USGS, NEED TO SET
C      BOTH ITRH AND JTRH BIG. TRY THE COMMENTED PARAMETER LINE FIRST.
C      THIS WILL REQUIRE APPROXI 0.9 GB MEMORY ON A 32-BIT IEEE MACHINE.
C      AN ESTIMATE OF THE DIMENSION SIZE CAN BE MADE FROM Data30s/rdem.out
C      AFTER THE FIRST JOB FAILS. USE (XMAXLAT-XMINLAT)*120 TO ESTIMATE
C      ITRH, AND (XMAXLON-XMINLON)*120 TO ESTIMATE JTRH.
C
C       PARAMETER (ITRH =  500, JTRH =  500, NOBT = ITRH*JTRH)
      PARAMETER (ITRH = 1500, JTRH = 1800, NOBT = ITRH*JTRH)
EOF
#
# ---------------------------------------------------------------
#          2. Set up NAMELIST
# ---------------------------------------------------------------
#
if ( -e terrain.namelist ) rm terrain.namelist
cat > terrain.namelist << EOF
 &MAPBG
 PHIC  =   40.0,      ; CENTRAL LATITUDE (minus for southern hemesphere)
XLONC =  -100.0,      ; CENTRAL LONGITUDE (minus for western hemesphere)
 IEXP  =    .F.,      ; .T. EXPANDED COARSE DOMAIN, .F. NOT EXPANDED.
                      ; USEFUL IF RUNNING RAWINS/little_r
```

```
 AEXP  =   360.,      ; APPROX EXPANSION (KM)
 IPROJ = 'LAMCON',    ; LAMBERT-CONFORMAL MAP PROJECTION
 ;IPROJ = 'POLSTR',   ; POLAR STEREOGRAPHIC MAP PROJECTION
 ;IPROJ = 'MERCAT',   ; MERCATOR MAP PROJECTION
 &END
 &DOMAINS
 ;
 MAXNES =    5,       ; NUMBER OF DOMAINS TO PROCESS
 NESTIX =   43,   55,  100,  136,   133, 221,  ; GRID DIMENSIONS IN Y DIRECTION
 NESTJX =   53,   55,  100,  151,   141, 221,  ; GRID DIMENSIONS IN X DIRECTION
 DIS    =  108.,  36.,  12.,  4.0,  1.0, 1.0,  ; GRID DISTANCE
 NUMNC  =    1,    1,    2,    3,    4,   5,  ; MOTHER DOMAIN ID
 NESTI  =    1,    6,    6,   17,   43,  50,  ; LOWER LEFT I OF NEST IN MOTHER DOMAIN
 NESTJ  =    1,   24,    8,   25,   49,  50,  ; LOWER LEFT J OF NEST IN MOTHER DOMAIN
 RID    =  1.5,  1.5,  1.5,  3.1,  2.3,  2.3, ; RADIUS OF INFLUENCE IN GRID UNITS
(IFANAL=T)
 NTYPE  =    1,    3,    4,    6,    6,   6,  ; INPUT DATA RESOLUTION
 ;
 ;      1:  1 deg (~111 km) global terrain and landuse
 ;      2: 30 min ( ~56 km) global terrain and landuse
 ;      3: 10 min ( ~19 km) global terrain and landuse
 ;      4;  5 min (  ~9 km) global terrain and landuse
 ;      5;  2 min (  ~4 km) global terrain and landuse
 ;      6; 30 sec ( ~.9 km) global terrain and landuse
 ;
 NSTTYP=     1,    2,    1,    1,    1,   1,  ;  1 -- ONE WAY NEST, 2 -- TWO WAY
 NEST
 &END
 &OPTN
 IFTER   = .TRUE.,    ; .T.-- TERRAIN,  .F.-- PLOT DOMAIN MAPS ONLY
 DATASW  = .T.,       ; .T. user specify terrain and landuse resolution (ntype)
                      ; .F. terrain program choose the data resolution
 IFANAL  = .F.,       ; .T.-- OBJECTIVE ANALYSIS, .F.-- INTERPOLATION
 ISMTHTR =  2 ,       ;  1: 1-2-1 smoother, 2: two pass smoother/desmoother
 IFEZFUG = .F.,       ; .T. USE NCAR GRAPHICS EZMAP WATER BODY INFO TO FUDGE THE
 LAND USE
                      ; .F. USE LANDWATER MASK DATA
 IFTFUG  = .F.,       ; .T. DON'T DO EZFUDGE WITHIN THE USER-SPECIFIED
 ;                      LAT/LON BOXES, need to define namelist fudget
 IFFUDG  = .F.,       ; .T. POINT-BY-POINT FUDGING OF LANDUSE,
                      ;  need to define namelist fudge
 IPRNTD  = .F.,       ; PRINT OUT LAT. AND LON. ON THE MESH
 IPRTHT  = .F.,       ; PRINT OUT ALL PROCESSING FIELDS ON THE MESH
 IPRINT  =  0,        ; = 1: A LOT MORE PRINT OUTPUT IN terrain.print.out
 FIN     = 100., 100., 100., 100., 100., 100., ; CONTOUR INTERVAL (meter) FOR TERRAIN
HEIGHT PLOT
 ;TRUELAT1=91.,       ; TRUE LATITUDE 1
 ;TRUELAT2=91.,       ; TRUE LATITUDE 2, use this if IPROJ='LAMCON'
 IFILL   = .TRUE.,    ; .TRUE. --- color filled plots
 LSMDATA = .TRUE.,    ; .TRUE. --- Create the data for LSM
 VEGTYPE = 1,         ; LANDUSE DATA TYPE: =0: old 13 cat; =1: 24 cat USGS; =2:
16 cat SiB
 VSPLOT  = .TRUE.,    ; .TRUE. --- plot Vege., Soil, Vege. Frc. percentages.
 IEXTRA  = .FALSE.,   ; .TRUE. --- Create extra data for Pleim-Xiu LSM
 &END
 &FUDGE
 ; USE ONLY IF IFFUDG = .T., POINT-BY-POINT FUDGING OF LANDUSE,
; IFFUG FOR EACH OF THE NESTS: .F. NO FUDGING, .T. FUDGING
 IFFUG   = .F.,.F.,    ; FUDGE FLAGS
 ; NDFUG : THE NUMBER OF FUDGING POINTS FOR EACH OF NESTS
 NDFUG   = 0,0,
 ; LOCATION (I,J) AND LANDUSE VALUES FOR EACH OF THE NESTS
 ; NOTE: REGARDLESS OF IFFUG AND NDFUG, 200 VALUES MUST BE GIVEN FOR
 ;       EACH NEST, OR ELSE THE INDEXING WILL GET MESSED UP
 ; The example below is for two domains. Add more for domain 3 and up
 ;       if needed. Do not remove 0 values for domain 1 and/or 2 even
 ;       they are not used.
 ;
 IFUG(1,1)=  200*0,    ; I location for fudge points in domain 1
 IFUG(1,2)=  200*0,    ; I location for fudge points in domain 2
 JFUG(1,1)=  200*0,    ; J location for fudge points in domain 1
```

```
 JFUG(1,2)=  200*0,    ; J location for fudge points in domain 2
 LNDFUG(1,1)= 200*0,   ; land-use value at fudge points for domain 1
 LNDFUG(1,2)= 200*0,   ; land-use value at fudge points for domain 2
 &END
 &FUDGET
 ; USE ONLY IF IFTFUG=.T., WHICH MEANS TERRAIN WON'T DO EZFUDGE WITHIN
 ;    THE USER-SPECIFIED LAT/LON BOXES.  THIS OPTION IS USED WHEN THERE
 ;    ARE INLAND BODIES OF WATER THAT ARE DEFINED IN THE LAND USE
 ;    DATA SET BUT NOT IN THE EZMAP DATA SET.  THIS OPTION PREVENTS
 ;    THOSE BODIES OF WATER FROM BEING WIPED OUT BY EZFUDGE
 NFUGBOX = 2             ;  NUMBER OF SUBDOMAINS IN WHICH TO
 ;                          TURN OFF EZMAP LAND USE FUDGING
 STARTLAT=45.0,44.0,     ;  LATITUDES OF LOWER-LEFT CORNERS OF SUBDOMAINS
 ENDLAT  =46.5,45.0,     ;  LATITUDES OF UPPER-RIGHT CORNERS OF SUBDOMAINS
 STARTLON=-95.0,-79.8,   ;  LONGITUDES OF LOWER-LEFT CORNERS OF SUBDOMAINS
 ENDLON  =-92.6,-78.5,   ;  LONGITUDES OF UPPER-RIGHT CORNERS OF SUBDOMAINS
 &END
 &EZFUDGE
 ; USE ONLY IF IFEZFUG=.T., WHICH TURNS ON EZMAP WATER BODY FUDGING OF LANDUSE.
 ; USERS: FEEL FREE TO ADD ANY MORE LAKE SURFACE HEIGHTS THAT YOU'LL NEED.
 ; HTPS IS THE HEIGHT IN METERS AND THE INDEX OF HTPS CORRESPONDS TO THE ID
 ; OF THE 'PS' AREA IN THE FILE ezmap_area_ids.
 ;
 HTPS(441) =  -.001   ; Oceans  --  Do NOT change this one
 HTPS(550) =  183.    ; Lake Superior
 HTPS(587) =  177.    ; Lakes Michigan and Huron
 HTPS(618) =  176.    ; Lake St. Clair
 HTPS(613) =  174.    ; Lake Erie
 HTPS(645) =   75.    ; Lake Ontario
 HTPS(480) = 1897.    ; Lake Tahoe
 HTPS(500) = 1281.    ; Great Salt Lake
 &END
EOF
#
# ------------------------------------------------------------------------------
#
#                 END OF USER MODIFICATION
#
# ------------------------------------------------------------------------------
```

APPENDIX B: Basic `pregrid.csh`

This job deck is reproduced from `/met/ngammon/analyses/pregrid/082801b/pregrid.csh`.

```
###############################################################################
###############################################################################
####                                                                       ####
####   NOTE:  2000-06-06:                                                 ####
####          This version of the pregrid.csh shell script has some        ####
####          differences from prior versions.  Users who are familiar     ####
####          with earlier versions should pay special attention to the    ####
####          use of VT3D, VTSST, VTSNOW, and VTSOIL script variables,     ####
####          which are now interpreted as lists of one or more            ####
####          individual Vtable files.  For further information on this    ####
####          new script, see the HTML documentation files:                ####
####                 REGRID/pregrid/Doc/html/how_to_use_pregrid.html       ####
####                 REGRID/pregrid/Doc/html/Advanced_csh.html             ####
####                                                                       ####
###############################################################################
###############################################################################
#

#  set echo

#
# Put your input files for pregrid into the directory you specify as DataDir:
#

set DataDir = /met/ngammon/analyses/ncar/edas/caselinks

#
# Specify the source of 3-d analyses
#


#   set SRC3D = ON84  # Old ON84-formatted NCEP GDAS analyses
#  set SRC3D = NCEP  # Newer GRIB-formatted NCEP GDAS analyses
  set SRC3D = GRIB  # Many GRIB-format datasets


#  InFiles:  Tell the program where you have put the analysis files,
#  and what you have called them.   If SRC3D has the value "GRIB",
#  then the Vtables you specify below in the script variable VT3D will
#  be used to interpret the files you specify in the ${InFiles} variable.

   set InFiles = ( ${DataDir}/* )
#
# Specify the source of SST analyses
#

#  set SRCSST = ON84
#  set SRCSST = NCEP
#  set SRCSST = NAVY
  set SRCSST = $SRC3D

#
#  InSST: Tell the program where the files with SST analyses are.  Do
#  this only if SST analyses are coming from files not named above in
#  InFiles.  If SRCSST has the value "GRIB", then the Vtables you
#  specify below in the script variable VTSST will be used to interpret
#  the files you specify in the ${InSST} variable.
#

  set InSST = ( )

#
```

```
# Select the source of snow-cover analyses (entirely optional)
#

   set SRCSNOW = $SRC3D
#  set SRCSNOW = ON84
#  set SRCSNOW = GRIB

#  InSnow:  Set InSnow only if the snow-cover analyses are from files
#  not listed in InFiles.  If SRCSNOW has the value "GRIB", then the
#  Vtables you specify below in the script variable VTSNOW will be used
#  to interpret the files you specify in the ${InSnow} variable.

   set InSnow = ()

#
# Select the source of soil model analyses (entirely optional)
#

   set SRCSOIL = $SRC3D

#  InSoil:  Set InSoil only if the soil analyses are from files
#  not listed in InFiles.  If SRCSOIL has the value "GRIB", then the
#  Vtables you specify below in the script variable VTSOIL will be
#  used to interpret the files you specify in the ${InSoil} variable.

#   set InSoil = ()

#
#  Build the Namelist
#
if ( -e ./pregrid.namelist ) then
   rm ./pregrid.namelist
endif
cat << End_Of_Namelist | sed -e 's/#.*//; s/  *$//' > ./pregrid.namelist
&record1
#
# Set the starting date of the time period you want to process:
#
 START_YEAR  = 2000   # Year (Four digits)
 START_MONTH = 08     # Month ( 01 - 12 )
 START_DAY   = 23     # Day ( 01 - 31 )
 START_HOUR  = 12     # Hour ( 00 - 23 )

 END_YEAR  = 2000   # Year (Four digits)
 END_MONTH = 09     # Month ( 01 - 12 )
 END_DAY   = 02     # Day ( 01 - 31 )
 END_HOUR  = 12     # Hour ( 00 - 23 )
#
# Define the time interval to process.
#
 INTERVAL =  10800 # Time interval (seconds) to process.
                   # This is most sanely the same as the time interval for
                   # which the analyses were archived, but you can really
                   # set this to just about anything, and pregrid will
                   # interpolate in time and/or skip over time periods for
                   # your regridding pleasure.

/
End_Of_Namelist

#
#  Tell the pregrid programs which Vtables to use.  Do this only
#  if you have selected GRIB-formatted input using SRC___ = GRIB above.
#  The directories referenced here are relative to REGRID/pregrid/.
#
#  The Vtable files specified in VT3D will be applied to the files
#  specified in the InFiles variable.  Similarly, the Vtable files
#  specified in VTSST, VTSNOW, and VTSOIL will be applied to the files
#  listed above in InSST, InSNOW, and InSoil, respectively.
#
   set VT3D = ( grib.misc/Vtable.AWIP3D )
```

```
   set VTSST = ( grib.misc/Vtable.AWIPSST )
   set VTSNOW = ( grib.misc/Vtable.AWIPSNOW )
   set VTSOIL = ( grib.misc/Vtable.AWIPSOIL )

###########################################################################
###########################################################################
######                                                             ######
######                  END USER MODIFICATION                      ######
######                                                             ######
#########################################################
```

APPENDIX C: Basic REGRIDDER `namelist.input`

This namelist is for the REGRIDDER run for the 4 km grid. It is reproduced from `/met/ngammon/analyses/regridder/101601/namelist.input`.

```
&record1
 start_year                     =  2000
 start_month                    =    08
 start_day                      =    23
 start_hour                     =    12
 end_year                       =  2000
 end_month                      =    09
 end_day                        =    02
 end_hour                       =    12
 interval                       = 10800 /

&record2
 ptop_in_Pa                     = 5000
 new_levels_in_Pa               = 97500, 95000 , 92500 , 90000 ,
                                  80000 ,
                                  75000 ,
                                  65000 , 60000 ,
                                  55000 ,
                                  45000 ,
                                  35000
 sst_to_ice_threshold           = -9999
 linear_interpolation           = .FALSE. /

&record3
 root                           = '/met/ngammon/analyses/pregrid/082801b/FILE',
                                  '/met/ngammon/analyses/pregrid/082801b/SNOW_FILE',
                                  '/met/ngammon/analyses/pregrid/082801b/SOIL_FILE',
                                  '/met/ngammon/analyses/pregrid/082801b/SST_FILE'
 terrain_file_name             = '/met/ngammon/analyses/terrain/oc1501/TERRAIN_DOMAIN3'
/
 constants_full_name            = ' '

&record4
 print_echo                     = .FALSE. ,
 print_debug                    = .FALSE. ,
 print_mask                     = .FALSE. ,
 print_interp                   = .FALSE. ,
 print_link_list_store          = .FALSE. ,
 print_array_store              = .FALSE. ,
 print_header                   = .FALSE. ,
 print_output                   = .FALSE. ,
 print_file                     = .FALSE. ,
 print_f77_info                 = .TRUE. /
```

APPENDIX D: Basic INTERPF `namelist.input`

This namelist is from the INTERPF run for the 4 km grid. It is reproduced from `/met/ngammon/analyses/interpf/101701/namelist.input`.

```
&record0
 input_file     = '/met/ngammon/analyses/regridder/101601/REGRID_DOMAIN3' /   !
pressure-level data file name

&record1
 start_year     =  2000                                ! The starting and
 start_month    =    08                                ! ending dates to
 start_day      =    23                                ! process
 start_hour     =    12
 end_year       =  2000
 end_month      =    09
 end_day        =    02
 end_hour       =    12
 interval       = 10800                                ! time difference (s)
 less_than_24h  = .FALSE. /                            ! if input is less than 24h

&record2
 sigma_f_bu     = 1.000,0.990,0.980,0.970,0.960,0.950,     ! full sigma, bottom-up,
                  0.940,0.930,0.920,0.910,0.895,0.880,     ! start with 1.0, end
                  0.865,0.850,0.825,0.800,0.775,0.750,     ! with 0.0
                  0.720,0.690,0.660,0.630,0.600,0.570,
                  0.540,0.510,0.475,0.440,0.405,0.370,
                  0.330,0.290,0.250,0.210,0.175,0.145,
                  0.115,0.090,0.065,0.045,0.025,0.010,
                  0.000
 ptop           = 5000                                ! top pressure if need to be
 redefined
 isfc           = 0 /                                  ! # sigma levels to spread
                                                       ! surface information

&record3
 p0             = 101300                               ! base state sea-level pres (Pa)
 tlp            = 45.                                ! base state lapse rate d(T)/d(ln P)
 ts0            = 304.                                 ! base state sea-level temp (K)
 tiso           = 200./                                  ! base state isothermal
stratospheric temp (K)

&record4
 removediv      = .TRUE.                               ! T/F remove integrated mean
divergence
 usesfc         = .TRUE.                               ! T/F use surface data
 wrth2o         = .TRUE. /                             ! T/F specific humidity wrt
 H2O

&record5
 ifdatim        = -1 /                                 ! # of IC time periods to output
```

APPENDIX E: Basic `configure.user`

The text below is excerpted from `/met/ngammon/output/oct25grid4/configure.user`.

```
#------------------------------------------------------------------------------
RUNTIME_SYSTEM = "SGI_Origin"
FC = f77
ABI = -n32 # 2 GB address space
#ABI = -64 # For 64-bit address space
IO = -mpio
PREC = # default 32-bit floating-point presicion.
#PREC = -r8 # 64-bit floating-point precision.
#Conversion program between different precisions of mminput and bdyout available
 from wesley@sgi.com
MP = -mp -MP:old_mp=OFF
#MP = -mp -MP:open_mp=OFF # Use SGI multiprocessing directives
OPT = -O3 -OPT:roundoff=3:IEEE_arithmetic=3 -OPT:reorg_common=OFF
#debugging#OPT = -g -DEBUG:div_check:subscript_check=ON:trap_uninitialized=ON
#select appropriate XLOCAL loader
#XLOCAL0 =
## Burk-Thompson PBL (IBLTYP=3) option mp directives
#XLOCAL0 = -Wl,-Xlocal,bt1_,-Xlocal,blk1_,-Xlocal,blk2_
## OSU LSM (ISOIL=2) option mp directives
XLOCAL0 = -Wl,-Xlocal,rite_,-Xlocal,abci_
## Gayno-Seaman PBL (IBLTYP=6) option mp directives
#XLOCAL0 = -Wl,-Xlocal,fog1d_,-Xlocal,surface1_,-Xlocal,surface2_,-Xlocal,surface3_,-
Xlocal,comsurfslab_
FCFLAGS = -I$(LIBINCLUDE) -D$(RUNTIME_SYSTEM) $(ABI) $(IO) $(PREC) $(MP) $(OPT)
CFLAGS =
CPP = /usr/lib/cpp
CPPFLAGS = -I$(LIBINCLUDE) -C -P
LDOPTIONS = $(ABI) $(PREC) $(MP) $(OPT) $(XLOCAL0)
LOCAL_LIBRARIES = -lfastm
MAKE = make -i -r -P                                          #--------------------
-------------------------------------------------------
# 4. General commands
#------------------------------------------------------------------------------
AR = ar ru
RM = rm -f
RM_CMD = $(RM) *.CKP *.ln *.BAK *.bak *.o *.i core errs ,* *~ *.a \
.emacs_* tags TAGS make.log MakeOut *.f !
GREP = grep -s
CC = cc
#------------------------------------------------------------------------------
# 5. Options for making ./include/parame.incl
#------------------------------------------------------------------------------
#
# FDDAGD (integer)                - "1" -> FDDA gridded run
FDDAGD = 1
#
# FDDAOBS (integer)               - "1" -> FDDA obs run
FDDAOBS = 0
#
# MAXNES (integer)                - Max Number of Domains in simulation
MAXNES = 4
#
# MIX,MJX (integer)               - Maximum Dimensions of any Domain
MIX = 136
MJX = 151
# MKX (integer)                   - Number of half sigma levels in model
MKX = 42
#------------------------------------------------------------------------------
# 6. Physics Options
#    The first MAXNES values in the list will be used for the corresponding
#        model nests; the rest in the list can be used to compile other options.
#        The exception is FRAD, of which only the first value is used in the model,
#        (i.e., only one radiation option is used for all nests). The rest allow
```

```
#        other options to be compiled.
#-----------------------------------------------------------------------------
# IMPHYS - for explicit moisture schemes (array,integer)
IMPHYS = "4,4,4,4,4,1,1,1,1,1"
#                                  - Dry,stable,warm rain,simple ice,mi phase,
#                                  - 1  ,2     ,3        ,4         ,5
#                                  - graupel(gsfc),graupel(reisner2),schultz
#                                  -,6            ,7                ,8
MPHYSTBL = 1
#                                  - 0=do not use look-up tables for moist
#                                    physics
#                                  - 1=use look-up tables for moist physics
#                                    (currently only simple ice and mix phase
#                                     are available)
#
# ICUPA - for cumulus schemes (array,integer)
#                                  - None,Kuo,Grell,AS,FC,KF,BM - 1,2,3,4,5,6,7
ICUPA  = "3,3,3,1,1,1,1,1,1,1"
#
# IBLTYP - for planetary boundary layer (array,integer)
#                                  - 0=no PBL fluxes,1=bulk,2=Blackadar,
#                                    3=Burk-Thompson,4=Eta M-Y,5=MRF,
#                                    6=Gayno-Seaman
IBLTYP  = "5,5,5,5,5,0,0,0,0,0"
#
# FRAD - for atmospheric radiation (integer)
#                                  - Radiation cooling of atmosphere
#                                    0=none,1=simple,2=cloud,3=ccm2
FRAD = "4,4,4,4,4"
#
# ISOIL - for multi-layer soil temperature model (integer)
#                                  - 0=no,1=yes (only works with IBLTYP=2,4,5,6)
#                                    2=OSU land-surface scheme (IBLTYP=5)
ISOIL = 1
#
# ISHALLO (array,integer)          - Shallow Convection Option
#                                    1=shallow convection,0=No shallow convection
ISHALLO  = "1,1,1,1,0,0,0,0,0,0"
#-----------------------------------------------------------------------------
# 7. MPP options
#
# For general information and updated "helpdesk" information see
#    http://www.mmm.ucar.edu/mm5/mpp
#    http://www.mmm.ucar.edu/mm5/mpp/helpdesk
#
#-----------------------------------------------------------------------------
#
#                                Presently, of the MPP platforms only the "sp2"
#                                is supplied with the "make deck" capability.
#
# MPP Software Layer
MPP_LAYER=RSL
#MPP_LAYER=NNTSMS
#
# PROCMIN_NS - minimum number of processors allowed in N/S dim
#
PROCMIN_NS = 1
#
# PROCMIN_EW - minimum number of processors allowed in E/W dim
#
PROCMIN_EW = 1
#
# ASSUME_HOMOGENOUS_ENVIRONMENT - on a machine with a heterogeneous
# mix of processors (different speeds) setting this compile time
# constant to 0 (zero) allows the program to detect the speed of each
# processor at the beginning of a run and then to attempt to come up with
# an optimal (static) mapping.  Set this to 0  for a heterogeneous
# mix of processors, set it to 1 for a homogeneous mix.  Unless you
# are certain you have a heterogeneous mix of processors, leave this
# set to 1.  Currently, this option is ignored on platforms other
```

```
# than the IBM SP.
#
ASSUME_HOMOGENEOUS_ENVIRONMENT = 1
#
```

APPENDIX F: Basic mm5.deck

Below is the deck used for the Oct25grid4 model run, found in /met/ngammon/output/oct25grid4/mm5.deck.

```
#!/bin/sh
#
#  Version 3 of mm5 job deck
#
#  Set the stack
#
limit stacksize unlimited
#
#  Set the multiprocessor options
#
OMP_NUM_THREADS=8
export OMP_NUM_THREADS
#     -<number_of_processors>
_DSM_PLACEMENT=ROUND_ROBIN
export _DSM_PLACEMENT

#    - For parallel execution on a processor set without contention:
#_DSM_WAIT=SPIN
#export _DSM_WAIT
#OMP_DYNAMIC=FALSE
#export OMP_DYNAMIC
#MPC_GANG OFF
#export MPC_GANG

#    - For parallel execution on a contented set of processors:
_DSM_WAIT=YEILD
export _DSM_WAIT
OMP_DYNAMIC=TRUE
export OMP_DYNAMIC
MPC_GANG=OFF
export MPC_GANG
#
#  The mm5 executable (mm5.exe) expects to find the following files
#      in the Run/ directory:
#      MMINPUT_DOMAIN1   -|
#      BDYOUT_DOMAIN1     | --> output files from Interpf
#      LOWBDY_DOMAIN1    -|
#      TERRAIN_DOMAIN[2,3..] if running nests  --> output from Terrain
#
#  If it is a restart run:
#      RESTART_DOMAIN1[,2,3..]  --> output from MM5 run: renamed from
#                                   SAVE_DOMAIN1[,2,3...]
#
#  If it is gridded FDDA run with surface analysis nudging:
#      SFCFDDA_DOMAIN1[2,3,...]
#
#  If it is observational nudging run:
#      MM5OBS_DOMAIN1[,2,3..]   --> user-created observation files
#
#  Output from a MM5 run:
#    If IFTAPE = 1
#      MMOUT_DOMAIN1[,2,3...]   --> one output for each domain
#    If IFSAVE = TRUE
#      SAVE_DOMAIN1[,2,3...]
#
#
# temp files should be accessible
umask 022
echo charge
#
# Select appropriate FDDAsw if doing gridded analysis FDDA
#
#FDDAsw=yes               # gridded FDDA input switch
```

```
FDDAsw=no
#
# Sections
# 1. Options for namelist ("mmlif")
# 2. Running...
#
#-------------------------------------------------------------------------------
# 1. Options for namelist ("mmlif")
#-------------------------------------------------------------------------------
#
#       The first dimension (column) of the arrays denotes the domain
#       identifier.
#               Col 1 = Domain #1, Col 2 = Dom #2, etc.
#
cat > ./Run/oparam << EOF
 &OPARAM
 ;
 ;      ************* FORECAST TIME AND TIME STEP ******************
 ;
 TIMAX  = 14340.,         ; forecast length in minutes
 TISTEP = 10.,         ; coarse domain DT in model, use 3*DX
 ;
 ;      ************** OUTPUT/RESTART OPTIONS ***************
 ;
 IFREST = .FALSE.,      ; whether this is a restart
    IXTIMR  = 4320,      ; restart time in minutes
 IFSAVE = .TRUE.,       ; save data for restart
    SVLAST = .FALSE.,    ; T: only save the last file for restart
                         ; F: save multiple files
    SAVFRQ = 720.,       ; how frequently to save data (in minutes)
 IFTAPE = 1,             ; model output: 0,1
    TAPFRQ = 60.,      ; how frequently to output model results (in minutes)
    BUFFRQ = 2880.,        ; how frequently to split model output files (in minutes),
 ;                         ignored if < TAPFRQ
    INCTAP = 1,1,1,1,1,1,1,1,1,1,  ; multipliers of TAPFRQ for outputting
 IFSKIP = .FALSE.,      ; whether to skip input files - DO NOT use this for restart
    CDATEST = '2000-08-23_12:00:00', ; the DATE for the starting file
 IFPRT = 0,             ; sample print out: =1, a lot of print
 PRTFRQ = 720.,         ; Print frequency for sample output (in minutes)
 MASCHK = 99999,        ; mass conservation check (KTAU or no. of time steps)
 IFTSOUT = .TRUE.,     ; output time series (default 30 points)
   TSLAT = 0.0,0.0,0.0,0.0,0.0, ; latitudes of time series points (S is negative)
   TSLON = 0.0,0.0,0.0,0.0,0.0, ; longitudes of time series points (W is negative)
 &END
EOF
cat > ./Run/lparam << EOF
 &LPARAM
 ;
 ;       1. user-chosen options I
 ;
RADFRQ    = 30.,  ;atmospheric radiation calculation frequency (in minutes)
 IMVDIF    = 1,    ;moist vertical diffusion in clouds - 0, 1 (IBLTYP=2,5 only)
 IVQADV    = 1,    ;vertical moisture advection uses log interpolation - 0, linear - 1
 IVTADV    = 1,    ;vertical temperature advection uses theta interpolation - 0,
 linear - 1
 ITHADV    = 1,    ;advection of temperature uses potential temperature - 1, standard - 0
 ITPDIF    = 1,    ;diffusion using perturbation temperature - 0,1
 ICOR3D    = 1,    ;3D Coriolis force - 0, 1
 IFUPR     = 0,    ;upper radiative boundary condition - 0, 1
 ;
 ;       2. do not change IBOUDY
 ;
 IBOUDY = 3, 2, 2, 2, 2, 2, 2, 2, 2, 2, ;boundary conditions
 ;        (fixed, time-dependent, relaxation -0,2,3)
 ;
 ;       3. keep the following 8 variables as they are
 ;          unless doing sensitivity runs
 ;
 IFDRY  = 0,                            ;fake-dry run (no latent heating) - 0, 1
 ;                                       for IMPHYS = 2,3,4,5,6,7 (requires ICUPA = 1)
 ISSTVAR= 0,                            ;varying SST in time - 1, otherwise, 0
```

```
 IMOIAV = 0, 0, 0, 0, 0, 0, 0, 0, 0, 0, ;bucket soil moisture scheme. 0 - not used,
                                        ;1 - used w/o extra input, 2 - user w/ soil m
input
 IFSNOW = 0, 0, 0, 0, 0, 0, 0, 0, 0, 0, ;SNOW COVER EFFECTS - 0, 1
 ;        (only if snow data are generated in DATAGRID)
 ISFFLX = 1, 1, 1, 1, 1, 1, 1, 1, 1, 1, ;surface fluxes - 0, 1
 ITGFLG = 1, 1, 1, 1, 1, 1, 1, 1, 1, 1, ;surface temperature prediction - 1:yes, 3:no
 ISFPAR = 1, 1, 1, 1, 1, 1, 1, 1, 1, 1, ;surface characteristics - 0, 1
 ICLOUD = 1, 1, 1, 1, 1, 1, 1, 1, 1, 1, ;cloud effects on radiation - 0, 1
 ;                                       currently for IFRAD = 1,2
 IEVAP  = 1, 1, 1, 1, 1, 1, 1, 1, 1, 1, ;evap of cloud/rainwater - <0, 0, >0
 ;                                       (currently for IMPHYS=3,4,5 only)
 ISMRD  = 0,                            ;soil moisture initialization by PX LSM:
 ;                                       =0, use moisture avail from LANDUSE.TBL
;
 ;                                       =2, use soil moisture from REGRID
 ;
EOF
cat > ./Run/nparam << EOF
 &NPARAM
 ;
 ;      ************** NEST AND MOVING NEST OPTIONS ***************
 ;
 LEVIDN =   0,1,2,3,4,1,1,1,1,1,               ; level of nest for each domain
 NUMNC  =   1,1,2,3,4,1,1,1,1,1,               ; ID of mother domain for each nest
 NESTIX =  136,  133, 73,  46,  46,  46,  46,  46,  ; domain size i
 NESTJX =  151,  141,  61,  61,  61,  61,  61,  ; domain size j
 NESTI  =   1,   49,  17,  41,   1,   1,   1,   1,   1,  ; start location i
 NESTJ  =   1,   43,  25,  48,   1,   1,   1,   1,   1,  ; start location i
 XSTNES =  0.,  14400.,  14400.,  14400.,  14400.,  0.,  0.,  0.,  0.,  0., ; domain
initiation
 XENNES =14400.,14400.,14400.,14400.,14400.,720.,720.,720.,720.,720.; domain termination
 IOVERW =   1,   1,   2,   2,   2,   0,   0,   0,   0,   0,  ; overwrite nest input
;          0=interpolate from coarse mesh (for nest domains);
 ;          1=read in domain initial conditions
 ;          2=read in nest terrain file
 IACTIV =   1,   0,   0,   0,   0,   0,   0,   0,   0,   0,  ;
 ;          in case of restart: is this domain active?
 ;
 ;      ************* MOVING NEST OPTIONS ******************
 ;
 IMOVE  =   0,   0,   0,   0,   0,   0,   0,   0,   0,   0, ; move domain 0,1
 IMOVCO =   1,   1,   1,   1,   1,   1,   1,   1,   1,   1, ; 1st move #
 ;          imovei(j,k)=L, ; I-INCREMENT MOVE (DOMAIN J, MOVE NUMBER K) IS L
 IMOVEI =   0,   0,   0,   0,   0,   0,   0,   0,   0,   0, ; I move #1
            0,   0,   0,   0,   0,   0,   0,   0,   0,   0, ; I move #2
            0,   0,   0,   0,   0,   0,   0,   0,   0,   0, ; I move #3
            0,   0,   0,   0,   0,   0,   0,   0,   0,   0, ; I move #4
            0,   0,   0,   0,   0,   0,   0,   0,   0,   0, ; I move #5
 IMOVEJ =   0,   0,   0,   0,   0,   0,   0,   0,   0,   0, ; J move #1
            0,   0,   0,   0,   0,   0,   0,   0,   0,   0, ; J move #2
            0,   0,   0,   0,   0,   0,   0,   0,   0,   0, ; J move #3
            0,   0,   0,   0,   0,   0,   0,   0,   0,   0, ; J move #4
            0,   0,   0,   0,   0,   0,   0,   0,   0,   0, ; J move #5
 IMOVET =   0,   0,   0,   0,   0,   0,   0,   0,   0,   0, ; time of move #1
            0,   0,   0,   0,   0,   0,   0,   0,   0,   0, ; time of move #2
            0,   0,   0,   0,   0,   0,   0,   0,   0,   0, ; time of move #3
            0,   0,   0,   0,   0,   0,   0,   0,   0,   0, ; time of move #4
            0,   0,   0,   0,   0,   0,   0,   0,   0,   0, ; time of move #5
 IFEED  =  3,     ; no feedback; 9-pt weighted average; 1-pt feedback w/o smoothing /
                  ; light smoothing / heavy smoothing - 0,1,2,3, and 4
 &END
EOF
cat > ./Run/pparam << EOF
 &PPARAM
 ;
 ;      ************* MISCELLANEOUS OPTIONS *****************
 ;
 ; The values for the following 5 variables are only used if ISFPAR = 0
 ;     (i.e. only land/water surface catagories)
 ;
```

```
 ZZLND  = 0.1,          ; roughness length over land in meters
 ZZWTR  = 0.0001,       ; roughness length over water in meters
 ALBLND = 0.15,         ; albedo
 THINLD = 0.04,         ; surface thermal inertia
 XMAVA  = 0.3,         ; moisture availability over land as a decimal fractionof one
 ;
 CONF   = 1.0,          ; non-convective precipitation saturation threshold (=1: 100%)
 &END
EOF
```